Supplementary Information

Supplementary tables

Supplementary Table 1. Antibody information
Supplementary Table 2. Connectivity Map analysis result

Supplementary Figure Legends

Supplementary Fig. 1. Molecular docking of coxibs to human PROKR1
Top view of the predicted protein shows valdecoxib (VAL, blue), rofecoxib (ROFE, red), paracoxib (PARE, yellow) bound to a binding pocket surrounded by the transmembrane domain (TM) of PROKR1. The boxes on the right show the binding pose of valdecoxib (top), rofecoxib (middle), and parecoxib (bottom), and the interacting residues of PROKR1 are represented by single letter amino acid symbols (F: phenylalanine, G: glycine, R: arginine, T: threonine).

Supplementary Fig. 2. IP1 accumulation response in HEK293T cells
IP1 accumulation is measured using human PROKR1-overexpressing (TG) or deficient (KO) HEK293T cells at different concentrations of each compound. Values are mean ± SD, n = 3.

Supplementary Fig. 3. cAMP competition assay
MTT assay is conducted using PROKR1-overexpressing (TG) or PROKR1-deficient (KO) HEK293T cells. cAMP accumulation is measured using human PROKR1-overexpressing cells at different concentrations of each compound. Values are mean ± SD, n = 3. $^{**}p < 0.01$, $^{***}p < 0.001$ vs. 0.78 μM, one-way ANOVA followed by Dunnett's post-hoc test. EC_{99} is effective concentration 99.

Supplementary Fig. 4. Coxib-induced oxidative muscle fiber specification
A. Prokr1 signaling in C2C12 myotubes. Protein levels of Prokr1, phosphorylated Creb (pCreb), Nr4a2, Pgc1a, Tfam, and Myh7 are depicted. **B**. Immunocytochemistry of C2C12 myotubes. Green signals represent Myh7, blue for nuclei. Myh7 index is the Myh7-positive area divided by the nuclei count. Scale bar is 200 μm. **C**. Respiratory chain complex in C2C12 myotubes.

Protein levels of Ndufb8 (complex I: CI), Sdhb (CII), Uqcrc2 (CIII), Mtco1 (CIV), and Atp5a (CV) are depicted. **D**. Mitochondria mass in C2C12 myotubes. MitoTracker-positive area is divided by nuclei count. **E**. Fatty acid oxidation (FAO) activity in C2C12 myotubes. Y-axis indicates FAO activity (U/μg protein). Values are mean ± SD, n = 3. *$p < 0.05$, **$p < 0.01$, ***$p < 0.001$, ****$p < 0.0001$ vs. control group (CTRL), one-way ANOVA followed by Dunnett's post-hoc test (A, C, E) or Kruskal-Wallis test followed by Dunn's post-hoc test (B, D).

Supplementary Fig. 5. Western blotting of Prokr1 signaling molecules in C2C12 myotubes

Each protein symbol and MW were labelled on the left side of the panel. CTRL: vehicle control, PK2: prokineticin 2, DER: deracoxib, CEL: celecoxib.

Supplementary Fig. 6. Quantification of Myh4 and Myh2 in C2C12 myotubes

CTRL: vehicle control, PK2: prokineticin 2, DER: deracoxib, CEL: celecoxib. Values are mean ± SD, n = 3. *$p < 0.05$ vs. control group (CTRL), one-way ANOVA followed by Dunnett's post-hoc test.

Supplementary Fig. 7. Immunocytochemistry of Myh4 and Myh2 in C2C12 myotubes

Green signals represent Myh4 (top), Myh2 (bottom), and blue for nuclei. Myh index is the Myh-positive area divided by the nuclei count. Scale bar is 200 μm. CTRL: vehicle control, PK2: prokineticin 2, DER: deracoxib, CEL: celecoxib. Values are mean ± SD, n = 3. *$p < 0.05$, **$p < 0.01$ vs. control group (CTRL), one-way ANOVA followed by Dunnett's post-hoc test.

Supplementary Fig. 8. Total nuclei number and fusion index for C2C12 myotubes

Total nuclei number in a unit area, fusion index for Myh7-, Myh4-, and Myh2-positive myotubes are presented. CTRL: vehicle control, PK2: prokineticin 2, DER: deracoxib, CEL: celecoxib. Values are mean ± SD, n = 3. ****$p < 0.0001$ vs. control group (CTRL), one-way ANOVA followed by Dunnett's post-hoc test.

Supplementary Fig. 9. Mitochondrial mass in C2C12 myotubes

Red signals indicate mitochondria, green for F-actin, and blue for nuclei. Bar scale is 200 μm. CTRL: vehicle control, PK2: prokineticin 2, DER: deracoxib, CEL: celecoxib.

Supplementary Fig. 10. Western blotting of PROKR1 signaling molecules in HSKMC myotubes

Each protein symbol and MW were labelled on the left side of the panel. CTRL: vehicle control, PK2: prokineticin 2, DER: deracoxib, CEL: celecoxib.

Supplementary Fig. 11. Quantification of MYH4 and MYH2 in HSKMC myotubes

CTRL: vehicle control, PK2: prokineticin 2, DER: deracoxib, CEL: celecoxib. Values are mean ± SD, n = 3. *$p < 0.05$, **$p < 0.01$ vs. control group (CTRL), one-way ANOVA followed by Dunnett's post-hoc test.

Supplementary Fig. 12. Immunocytochemistry of MYH4 and MYH2 in HSKMC myotubes

Green signals represent MYH4 (top), MYH2 (bottom), and blue for nuclei. MYH index is the MYH-positive area divided by the nuclei count. Scale bar is 200 μm. CTRL: vehicle control, PK2: prokineticin 2, DER: deracoxib, CEL: celecoxib. Values are mean ± SD, n = 3. *$p < 0.05$ vs. control group (CTRL), one-way ANOVA followed by Dunnett's post-hoc test.

Supplementary Fig. 13. Total nuclei number and fusion index for HSKMC myotubes

Total nuclei number in a unit area, fusion index for MYH7-, MYH4-, and MYH2-positive myotubes are presented. CTRL: vehicle control, PK2: prokineticin 2, DER: deracoxib, CEL: celecoxib. Values are mean ± SD, n = 3. **$p < 0.01$, ***$p < 0.001$, ****$p < 0.0001$ vs. control group (CTRL), one-way ANOVA followed by Dunnett's post-hoc test.

Supplementary Fig. 14. Mitochondrial mass in HSKMC myotubes

Red signals indicate mitochondria, green for F-actin, and blue for nuclei. Bar scale is 200 μm. CTRL: vehicle control, PK2: prokineticin 2, DER: deracoxib, CEL: celecoxib.

Supplementary Fig. 15. Attenuation of celecoxib-induced oxidative muscle fiber specification in *Prokr1* knock-downed mouse myotubes

A. Attenuation of celecoxib-induced Prokr1 signaling activity. **B**. Attenuation of celecoxib-induced Myh7-postive myogenesis. Scale bar is 200 μm. CEL: celecoxib. Values are mean ± SD, n = 3. *$p < 0.05$, ***$p < 0.001$ vs. siRNA-scramble, one-way ANOVA followed by

Dunnett's post-hoc test.

Supplementary Fig. 16. Body composition of neonatal mice

Fat (red) and muscle distribution (blue) in mice by concentration using dual-energy X-ray absorptiometry (DEXA). The label at the top of each figure represents the concentration of celecoxib added in the diet. Scale bar is 3 cm.

Supplementary Fig. 17. Relative muscle weights and muscle fiber counts of neonatal mice

Bodyweight-relative gastrocnemius and soleus muscle weights (mg/g bw) and muscle fiber number per a unit area (0.44 μm^2) are presented. Values are mean ± SD, n = 3~4. *$p < 0.05$, **$p < 0.01$, ***$p < 0.001$ vs. 0 ppm, one-way ANOVA followed by Dunnett's post-hoc test.

Supplementary Fig. 18. Macroscopic examination of thigh muscle

Representative figures of different concentrations of celecoxib are presented. The concentration of celecoxib is indicated at the top of each figure (ppm). Scale bar is 1000 μm.

Supplementary Fig. 19. H&E staining of neonate muscle tissues

Representative figures of muscle tissue from male and female mice are shown. The concentration of celecoxib is indicated at the top of each figure. Scale bar is 100 μm.

Supplementary Fig. 20. Western blotting of Prokr1 signal molecules in male neonate muscle tissues

Each protein symbol and MW were labelled on the left side of the panel. The concentration of celecoxib is indicated at the top of each panel.

Supplementary Fig. 21. Western blotting of Prokr1 signal molecules in female neonate muscle tissues

Each protein symbol and MW were labelled on the left side of the panel. The concentration of celecoxib is indicated at the top of each panel.

Supplementary Fig. 22. Bodyweight changes of young adult mice

Each graph shows the weekly bodyweight change of male (left) and female mice (right) from 3 weeks old to 12 weeks old. Values are mean ± SD, n = 15. *$p < 0.05$, **$p < 0.01$, ***$p <$

0.001, ****$p < 0.0001$ vs. 0 ppm, one-way ANOVA followed by Dunnett's post-hoc test.

Supplementary Fig. 23. Food consumption of young adult mice

Each graph shows the daily food consumption of male (left) and female mice (right) from 3 weeks old to 12 weeks old. Values are mean ± SD, n = 15. *$p < 0.05$, **$p < 0.01$, ***$p < 0.001$, ****$p < 0.0001$ vs. 0 ppm, one-way ANOVA followed by Dunnett's post-hoc test.

Supplementary Fig. 24. Body composition of young adult mice

Fat (red) and muscle distribution (blue) in mice by concentration using dual-energy X-ray absorptiometry (DEXA). The label at the top of each figure represents the concentration of celecoxib added in the diet. Scale bar is 3 cm.

Supplementary Fig. 25. Glucose tolerance of young adult mice

Blood glucose levels during an oral glucose tolerance test (GTT) by concentration of celecoxib (ppm) are presented. Value is mean ± SD, n = 7. *$p < 0.05$ vs. 0 ppm, one-way ANOVA followed by Dunnett's post-hoc test.

Supplementary Fig. 26. Insulin tolerance of young adult mice

Blood glucose level during insulin tolerance test (ITT) by concentration of celecoxib (ppm) are presented. Value is mean ± SD, n = 7. *$p < 0.05$, **$p < 0.01$, ***$p < 0.001$, ****$p < 0.0001$ vs. 0 ppm, one-way ANOVA followed by Dunnett's post-hoc test.

Supplementary Fig. 27. Area under the glucose curve during ITT and basal (fasting) glucose levels of young adult mice

Area under the glucose concentration-time curve (AUC) during ITT and basal (fasting) glucose levels of young adult mice (12 weeks old) are presented. Value is mean ± SD, n = 3~4. *$p < 0.05$, **$p < 0.01$, ***$p < 0.001$, ****$p < 0.0001$ vs. 0 ppm, one-way ANOVA followed by Dunnett's post-hoc test.

Supplementary Fig. 28. Respiratory exchange ratio of young adult mice

The graph shows the respiratory exchange ratio (RER) by concentration of celecoxib (ppm) in male and female mice. White areas represent the light phase (8 am - 8 pm) and shaded areas for the dark phase (8 pm - 8 am).

Supplementary Fig. 29. Energy expenditure of young adult mice

Energy expenditure (EE) by concentration of celecoxib (ppm) in male and female mice are presented. White areas represent the light phase (8 am - 8 pm) and shaded areas for the dark phase (8 pm - 8 am).

Supplementary Fig. 30. Organ weights of young adult mice

A. Body weight-related organ weights. **B**. Absolute organ weights. White bar indicates 0 ppm of celecoxib, green for 300 ppm, blue for 700 ppm, and red for 1500 ppm. Values are mean ± SD, n = 4. *$p < 0.05$, **$p < 0.01$ vs. 0 ppm, one-way ANOVA followed by Dunnett's post-hoc test. Kruskal-Wallis test followed by Dunn's post-hoc text for male gastrocnemius muscle tissue, female soleus muscle tissue and liver weights, and one-way ANOVA followed by Dunnett's post-hoc test for others.

Supplementary Fig. 31. H&E staining of young adult mice muscle tissues

Representative figures of muscle tissue from male and female mice are shown. Animal sex, celecoxib concentration (ppm), and tissue are labeled in each figure. Scale bar is 100 μm. M: male, F: female, GAS: gastrocnemius muscle tissue, SOL: soleus muscle tissue.

Supplementary Fig. 32. Mitochondria mass in young adult mice muscle tissues

Histology shows the mitochondria (red) and nuclei (blue) of muscle fibers. The concentration of celecoxib is indicated at the top of each figure (ppm). Scale bar is 100 μm.

Supplementary Fig. 33. Lipid content in young adult mice muscle tissues

Qualitative and quantitative perilipin 2 (Plin2) expression levels in gastrocnemius muscle tissue of male and female young adult mice are presented. Green signal represents Plin2, blue for nuclei. Scale bar is 100 μm. M: male, F: female. Values are mean ± SD, n = 3. *$p < 0.05$ vs. 0 ppm, one-way ANOVA followed by Dunnett's post-hoc test

Supplementary Fig. 34. Western blotting of Prokr1 signaling molecules in male young adult mice muscle tissues

Each protein symbol and MW were labelled on the left side of the panel. The concentration of celecoxib is indicated at the top of each panel.

Supplementary Fig. 35. Western blotting of Prokr1 signaling molecules in female young adult mice muscle tissues

Each protein symbol and MW were labelled on the left side of the panel. The concentration of celecoxib is indicated at the top of each panel.

Supplementary Fig. 36. Bodyweight changes of adult mice

Each graph shows the weekly bodyweight change of male (left) and female mice (right) from 3 weeks old to 20 weeks old. Values are mean ± SD, n = 15. *$p < 0.05$, **$p < 0.01$, ***$p < 0.001$, ****$p < 0.0001$ vs. 0 ppm, Kruskal-Wallis test followed by Dunn's post-hoc text for male age (6, 7, 12, 13, 14, 15, 16, 17, 18, 19, 20 weeks) and one-way ANOVA followed by Dunnett's post-hoc test for others.

Supplementary Fig. 37. Food consumption of adult mice

Each graph shows the daily food consumption of male (left) and female mice (right) from 3 weeks old to 20 weeks old. Values are mean ± SD, n = 15. *$p < 0.05$, **$p < 0.01$, ***$p < 0.001$, ****$p < 0.0001$ vs. 0 ppm, Kruskal-Wallis test followed by Dunn's post-hoc text for male age (13,16, 17, 19, 20 weeks) and one-way ANOVA followed by Dunnett's post-hoc test for others.

Supplementary Fig. 38. Body composition of adult mice

Fat (red) and muscle distribution (blue) in mice by concentration using dual-energy X-ray absorptiometry (DEXA). The label at the top of each figure represents the concentration of celecoxib added in the diet. Scale bar is 2 cm.

Supplementary Fig. 39. Glucose tolerance of adult mice

Blood glucose levels during an oral glucose tolerance test (OGTT) by concentration of celecoxib (ppm) are presented. Value is mean ± SD, n = 7. *$p < 0.05$ vs. 0 ppm, one-way ANOVA followed by Dunnett's post-hoc test.

Supplementary Fig. 40. Insulin tolerance of adult mice

Blood glucose level during insulin tolerance test (UTT) by concentration of celecoxib (ppm) are presented. Value is mean ± SD, n = 7. *$p < 0.05$, **$p < 0.01$, ***$p < 0.001$, ****$p < 0.0001$ vs. 0 ppm, one-way ANOVA followed by Dunnett's post-hoc test.

Supplementary Fig. 41. Area under the glucose curve during ITT and basal (fasting) glucose levels of adult mice

Area under the glucose concentration-time curve (AUC) during ITT and basal (fasting) glucose levels of adult mice (20 weeks old) are presented. Value is mean ± SD, n = 3~4. *$p < 0.05$, **$p < 0.01$, ***$p < 0.001$, ****$p < 0.0001$ vs. 0 ppm, one-way ANOVA followed by Dunnett's post-hoc test.

Supplementary Fig. 42. Respiratory exchange ratio of adult mice

The graph shows the respiratory exchange ratio (RER) by concentration of celecoxib (ppm) in male and female mice. White areas represent the light phase (8 am – 8 pm) and shaded areas for the dark phase (8 pm – 8 am).

Supplementary Fig. 43. Energy expenditure of adult mice

Energy expenditure (EE) by concentration of celecoxib (ppm) in male and female mice are presented. White areas represent the light phase (8 am – 8 pm) and shaded areas for the dark phase (8 pm – 8 am).

Supplementary Fig. 44. Organ weights of adult mice

A. Body weight-related organ weights. **B**. Absolute organ weights. White bar indicates 0 ppm of celecoxib, green for 300 ppm, blue for 700 ppm, and red for 1500 ppm. Values are mean ± SD, n = 3. *$p < 0.05$, **$p < 0.01$ vs. 0 ppm, one-way ANOVA followed by Dunnett's post-hoc test. one-way ANOVA followed by Dunnett's post-hoc test.

Supplementary Fig. 45. H&E staining of adult mice muscle tissues

Representative figures of muscle tissue from male and female mice are shown. Animal sex, celecoxib concentration (ppm), and tissue are labeled in each figure. Scale bar is 100 μm. M: male, F: female, GAS: gastrocnemius muscle tissue, SOL: soleus muscle tissue.

Supplementary Fig. 46. Mitochondria mass in adult mice muscle tissues

Histology shows the mitochondria (red) and nuclei (blue) of muscle fibers. The concentration of celecoxib is indicated at the top of each figure (ppm). Scale bar is 100 μm.

Supplementary Fig. 47. Lipid content in adult mice muscle tissues

Qualitative and quantitative perilipin 2 (PLIN2) expression levels in gastrocnemius muscle tissue of male and female adult mice are presented. Green signal represents PLIN2, blue for nuclei. Scale bar is 100 μm. M: male, F: female. Values are mean ± SD, n = 3. *$p < 0.05$ vs. 0 ppm, one-way ANOVA followed by Dunnett's post-hoc test Values are mean ± SD, n = 3. **$p < 0.01$, ***$p < 0.001$ vs. 0 ppm, one-way ANOVA followed by Dunnett's post-hoc test

Supplementary Fig. 48. Western blotting of Prokr1 signaling molecules in male adult mice muscle tissues

Each protein symbol and MW were labelled on the left side of the panel. The concentration of celecoxib is indicated at the top of each panel.

Supplementary Fig. 49. Western blotting of Prokr1 signaling molecules in female adult mice muscle tissues

Each protein symbol and MW were labelled on the left side of the panel. The concentration of celecoxib is indicated at the top of each panel.

Supplementary Fig. 1

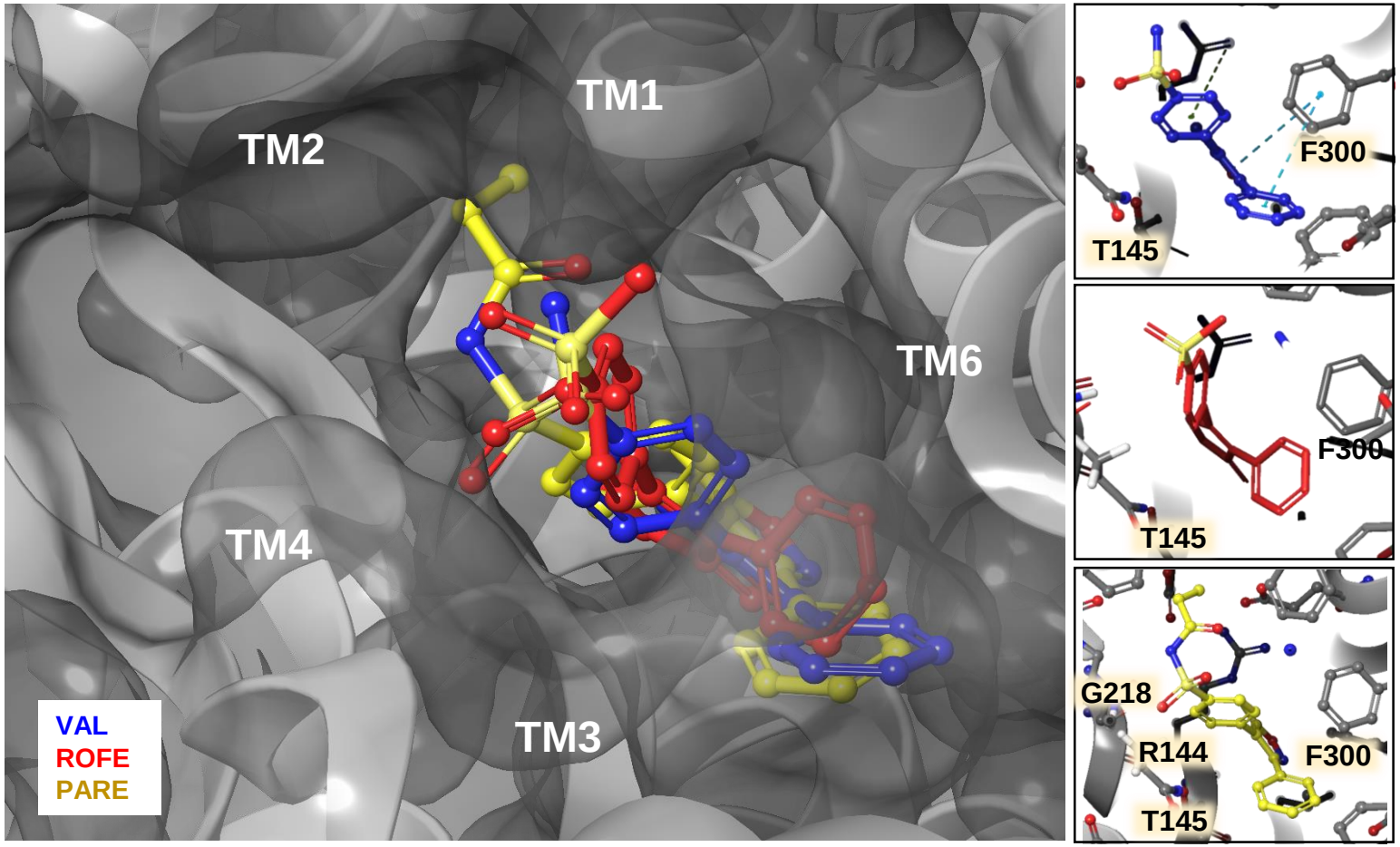

Supplementary Fig. 2

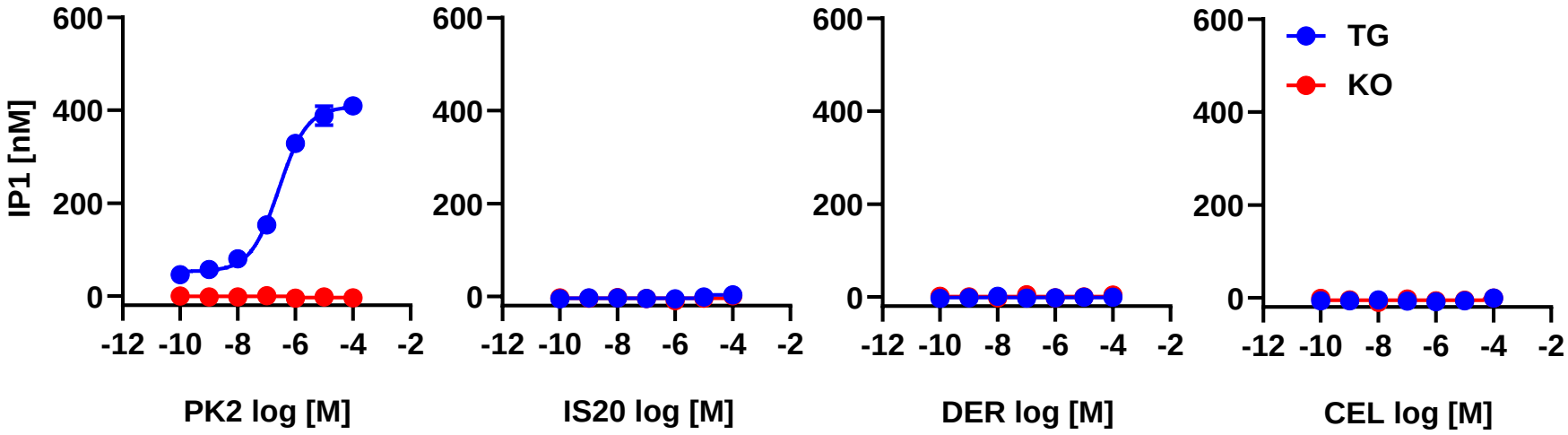

Supplementary Fig. 3

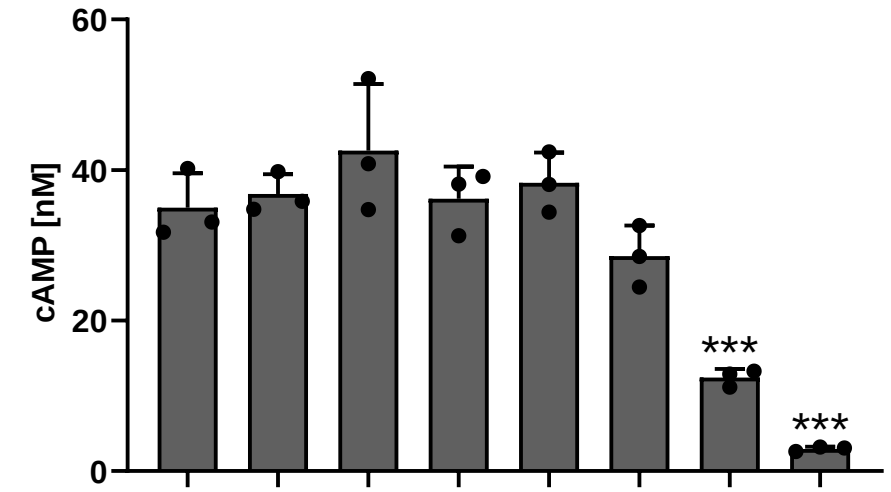

PK2	10 nM (EC_{99})							
IS20 (uM)	0.78	1.56	3.13	6.25	12.5	25	50	100

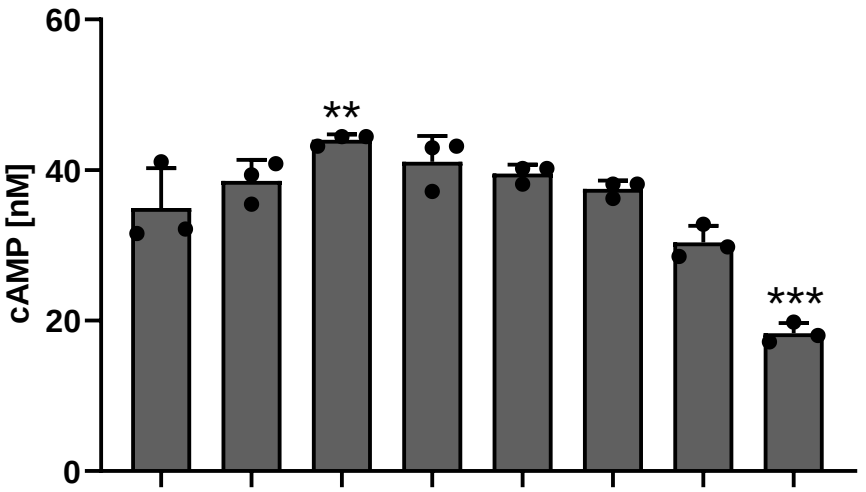

PK2	10 nM (EC_{99})							
CEL (uM)	0.78	1.56	3.13	6.25	12.5	25	50	100

Supplementary Fig. 4

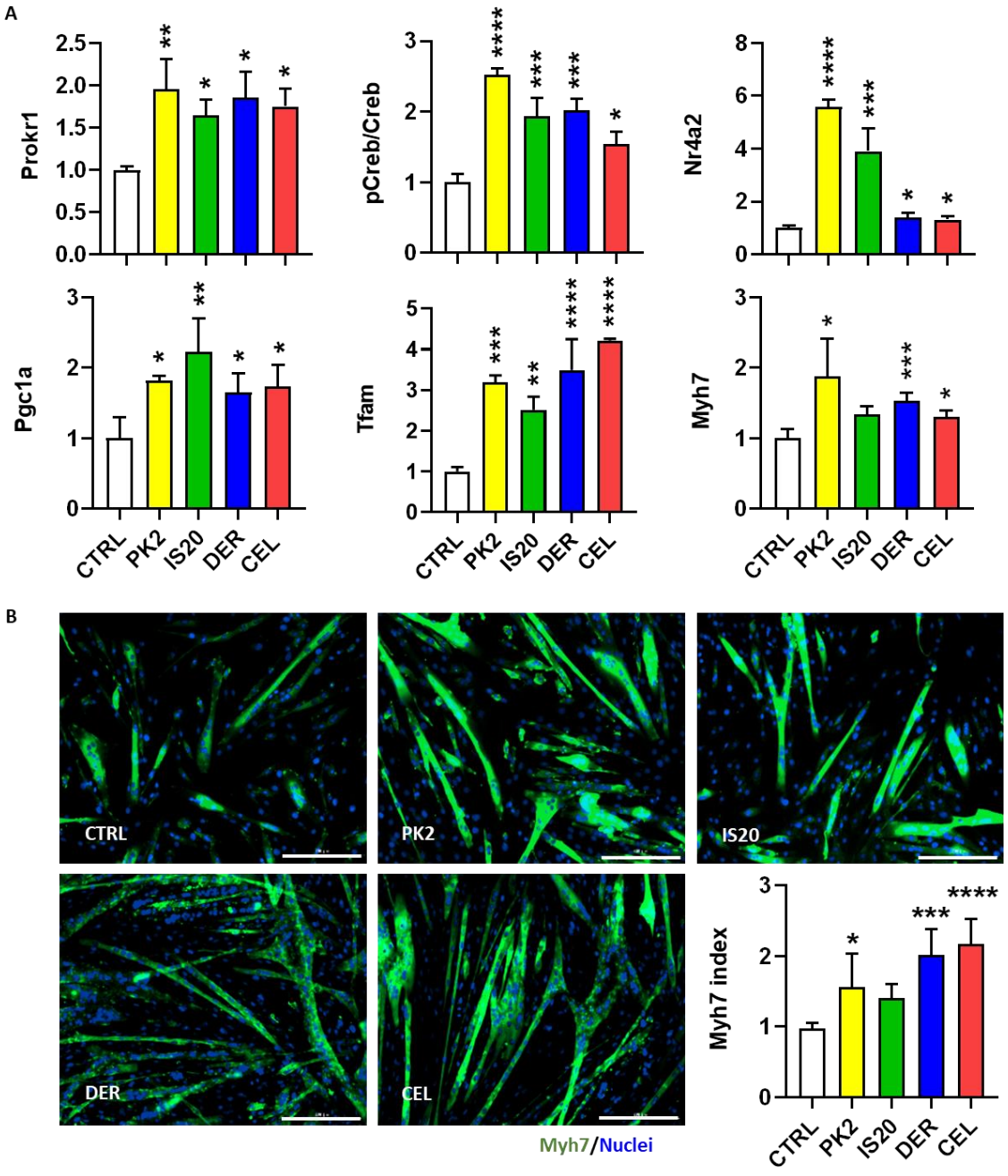

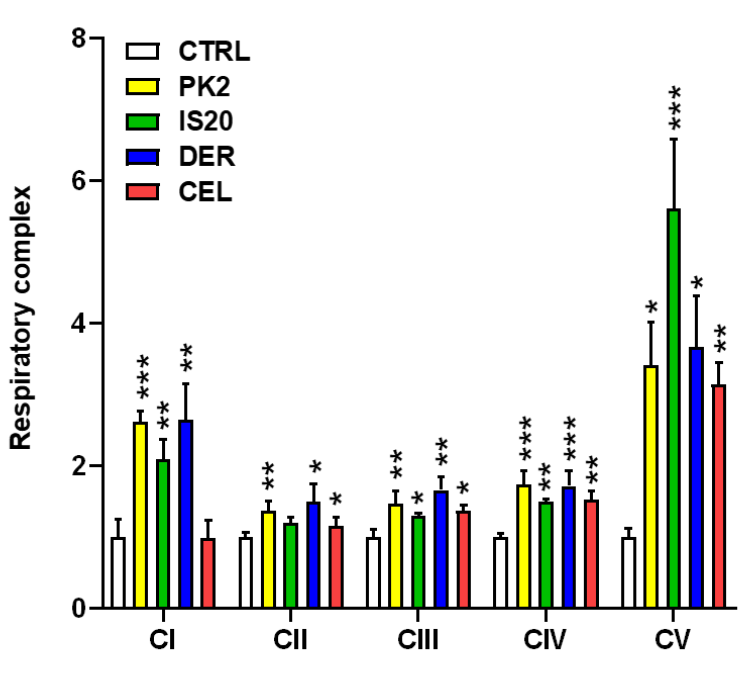

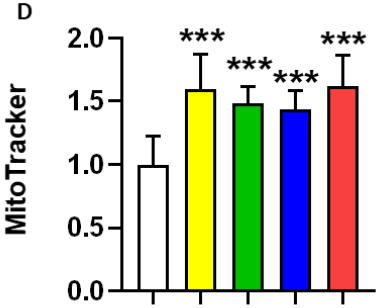

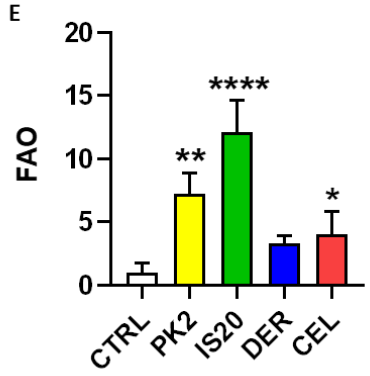

Supplementary Fig. 5

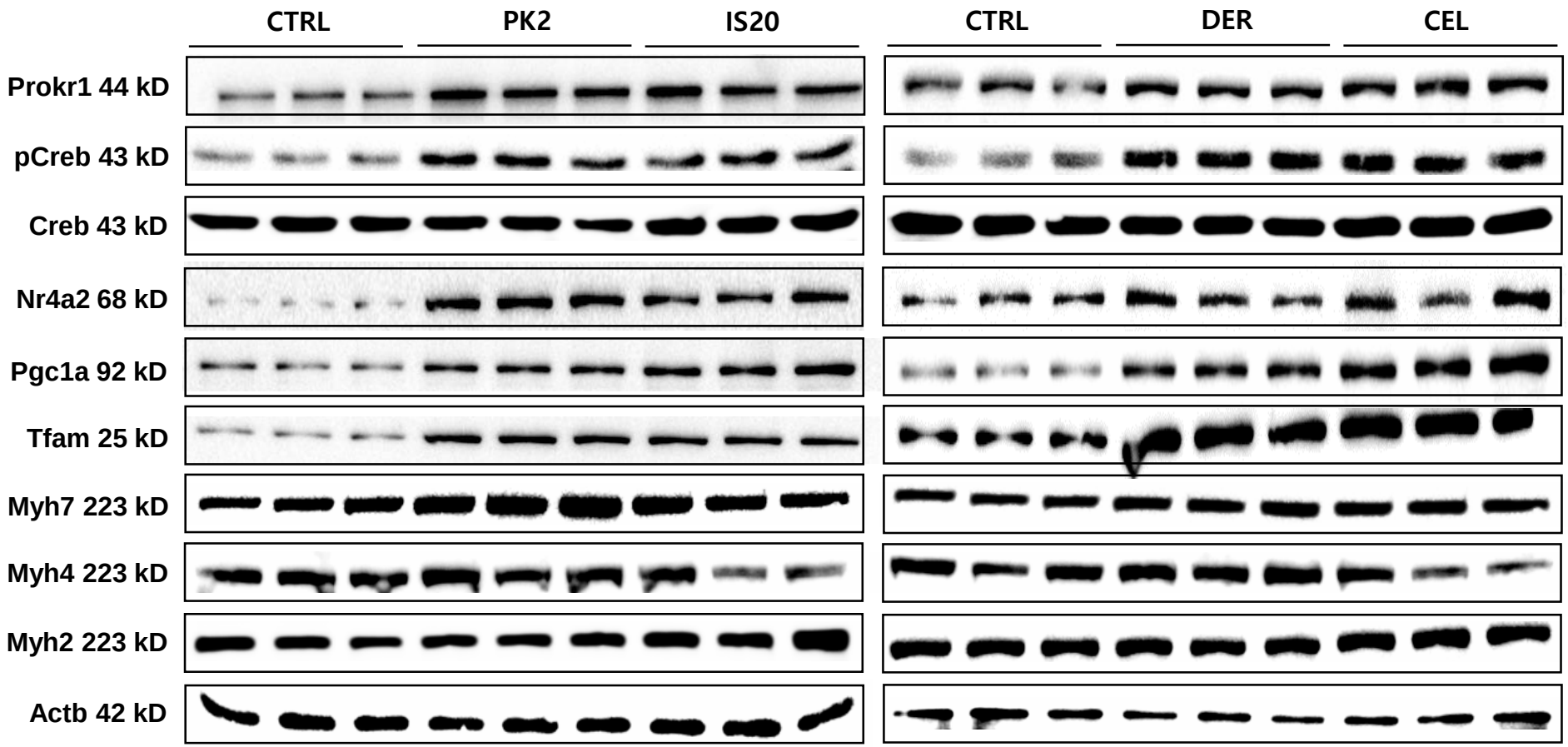

Supplementary Fig. 6

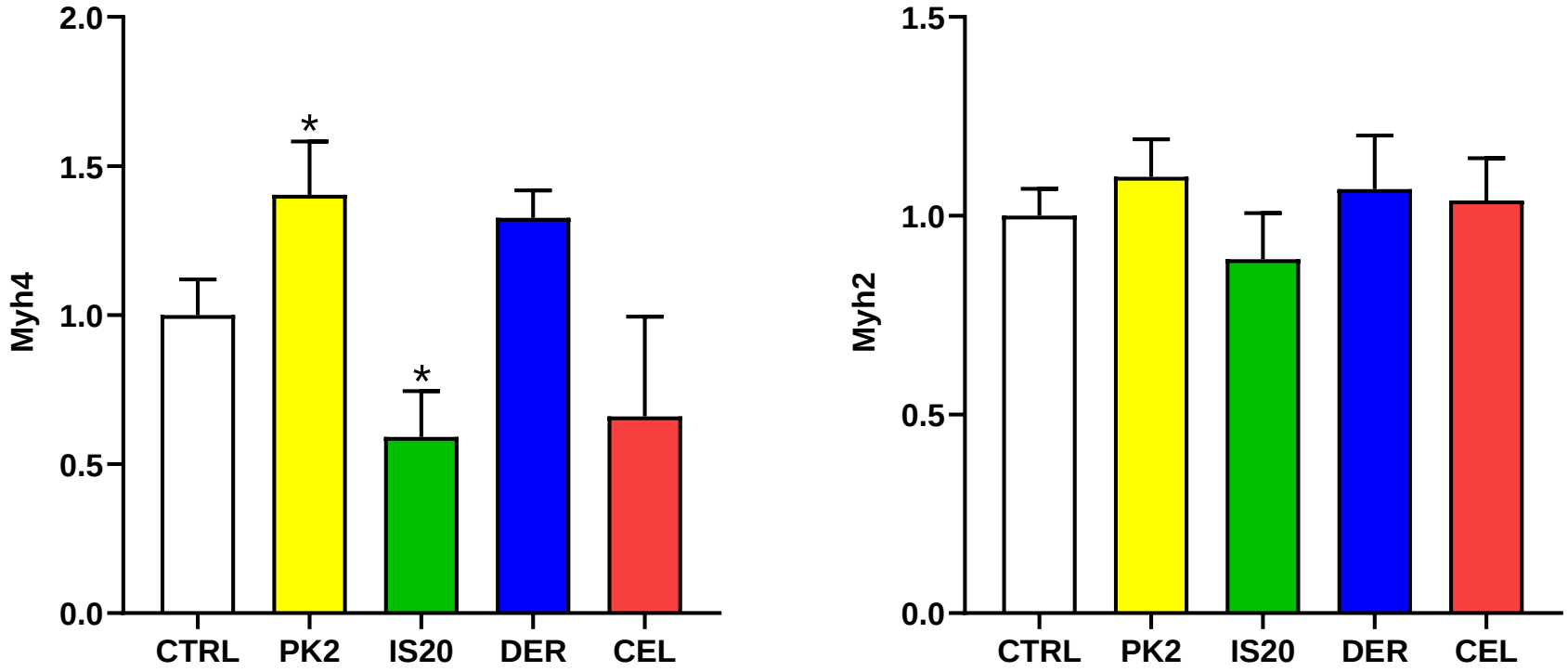

Supplementary Fig. 7

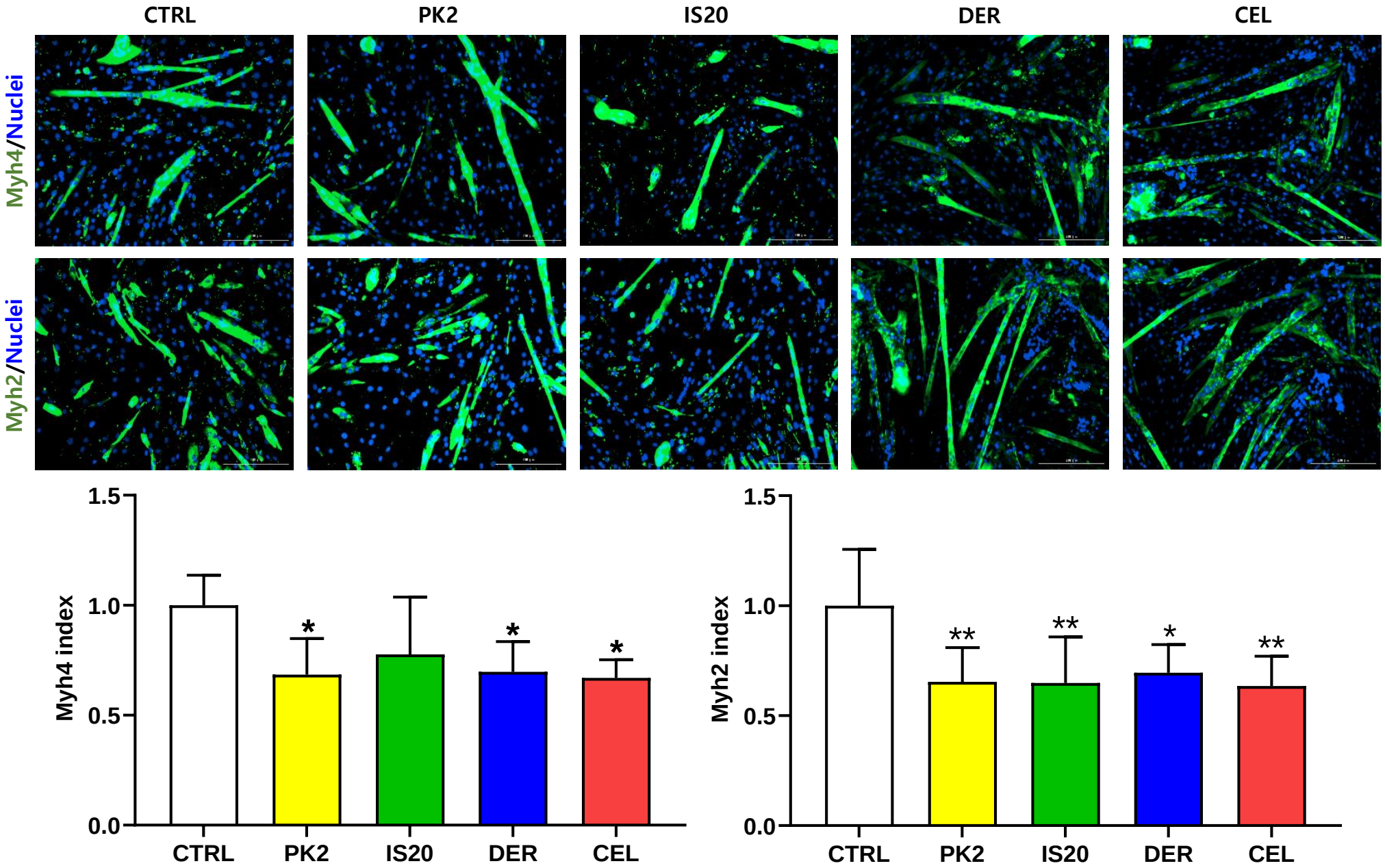

Supplementary Fig. 8

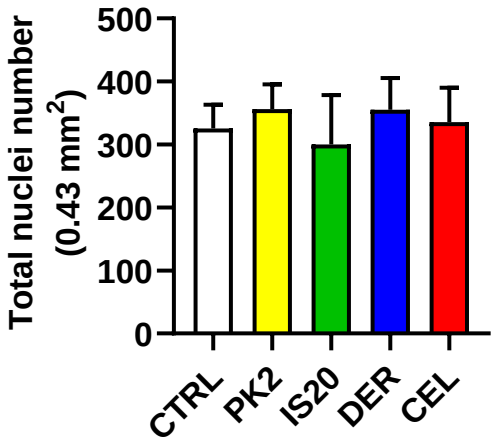

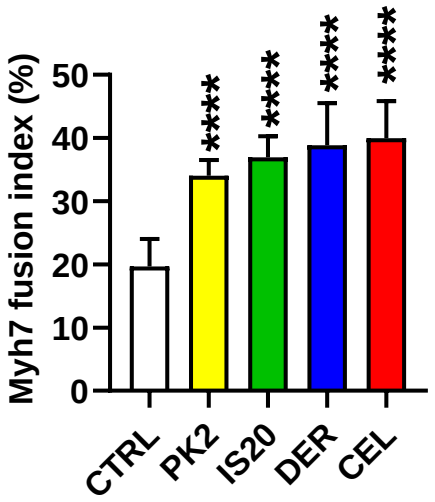

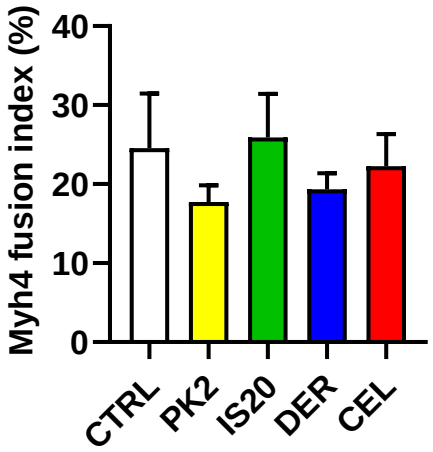

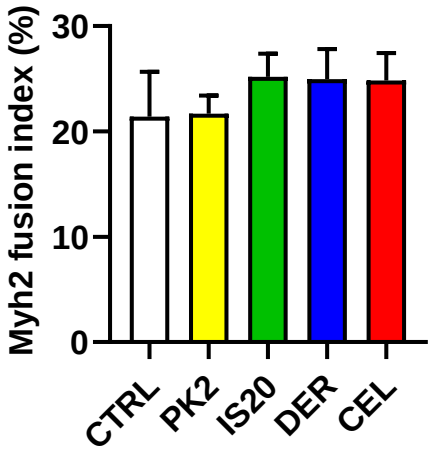

Supplementary Fig. 9

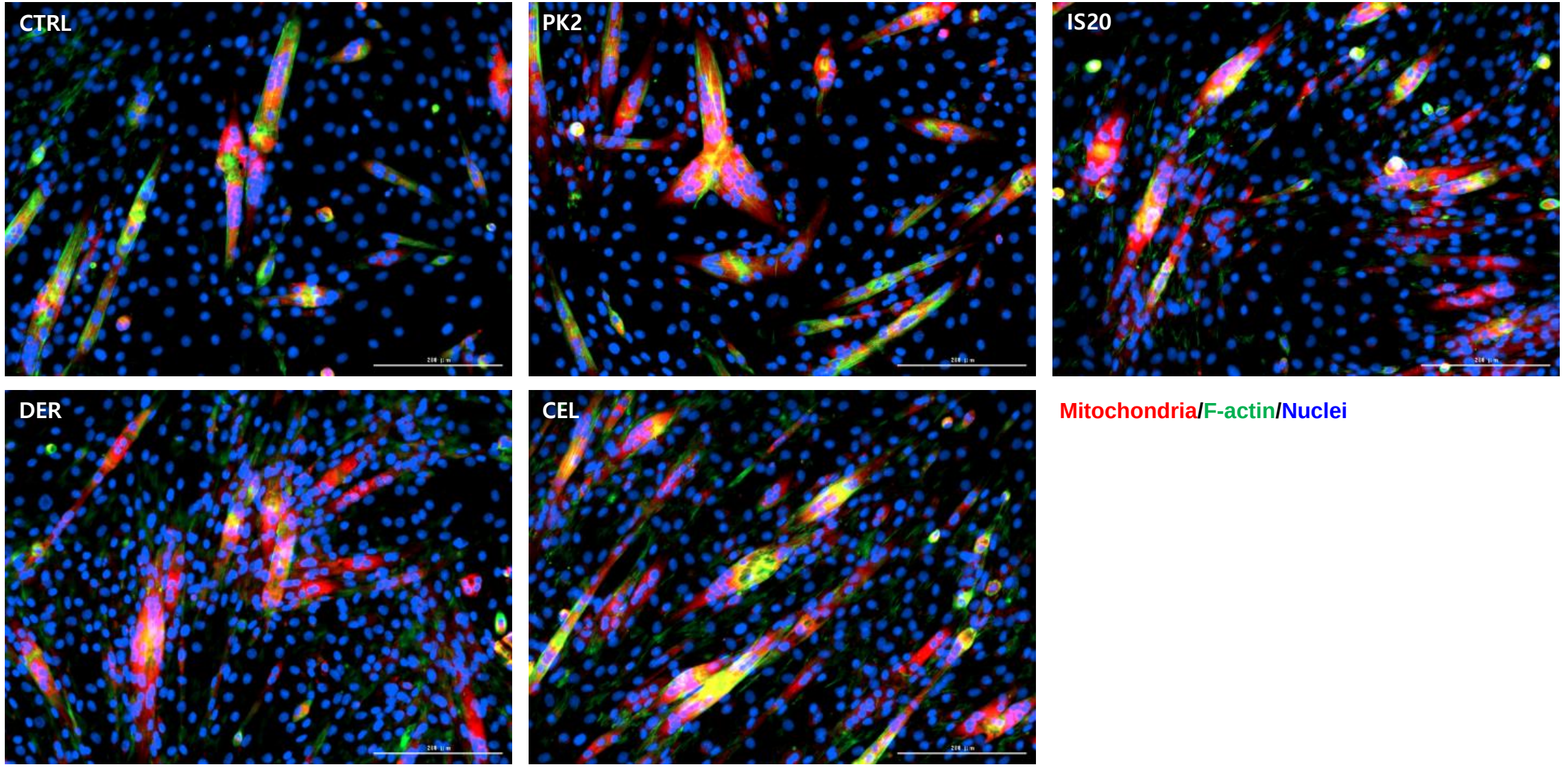

Supplementary Fig. 10

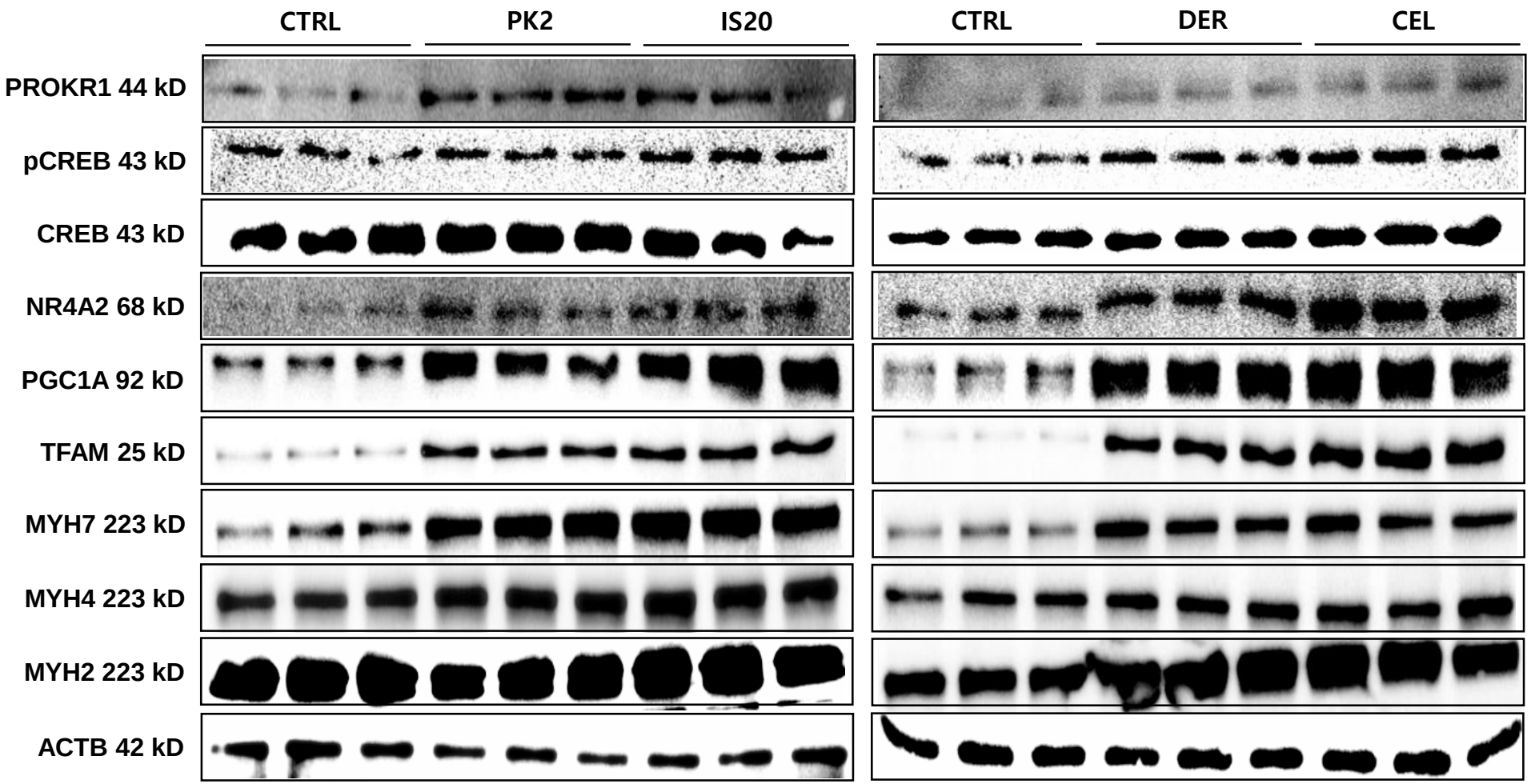

Supplementary Fig. 11

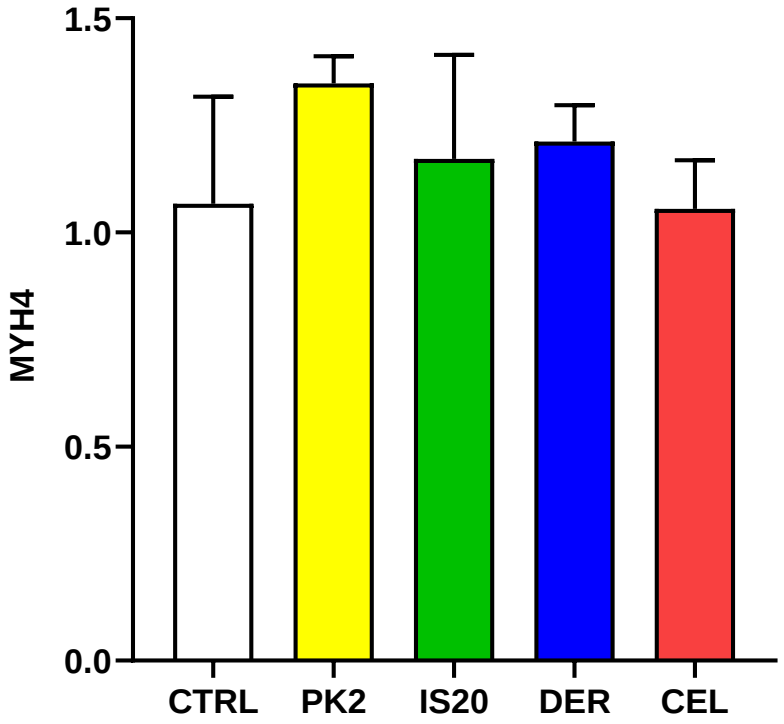

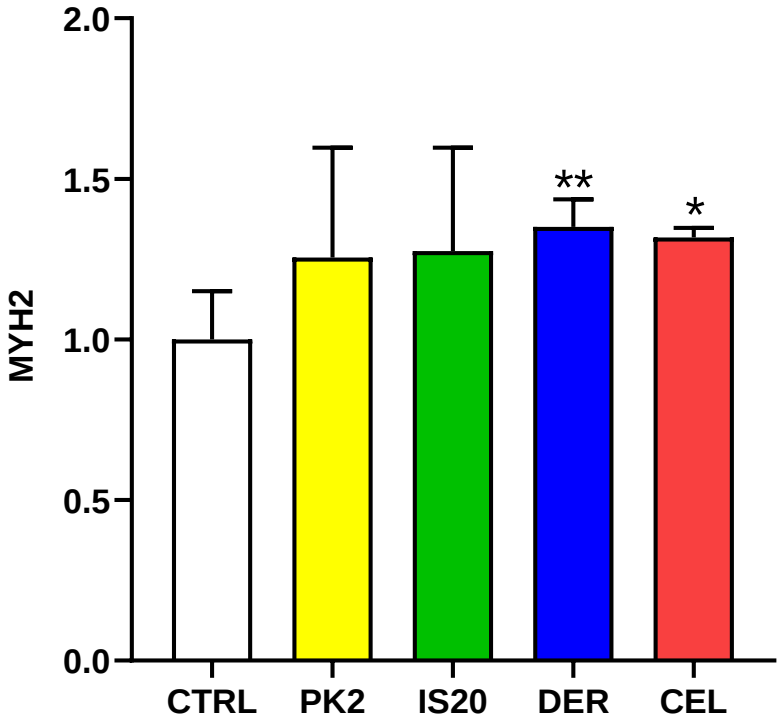

Supplementary Fig. 12

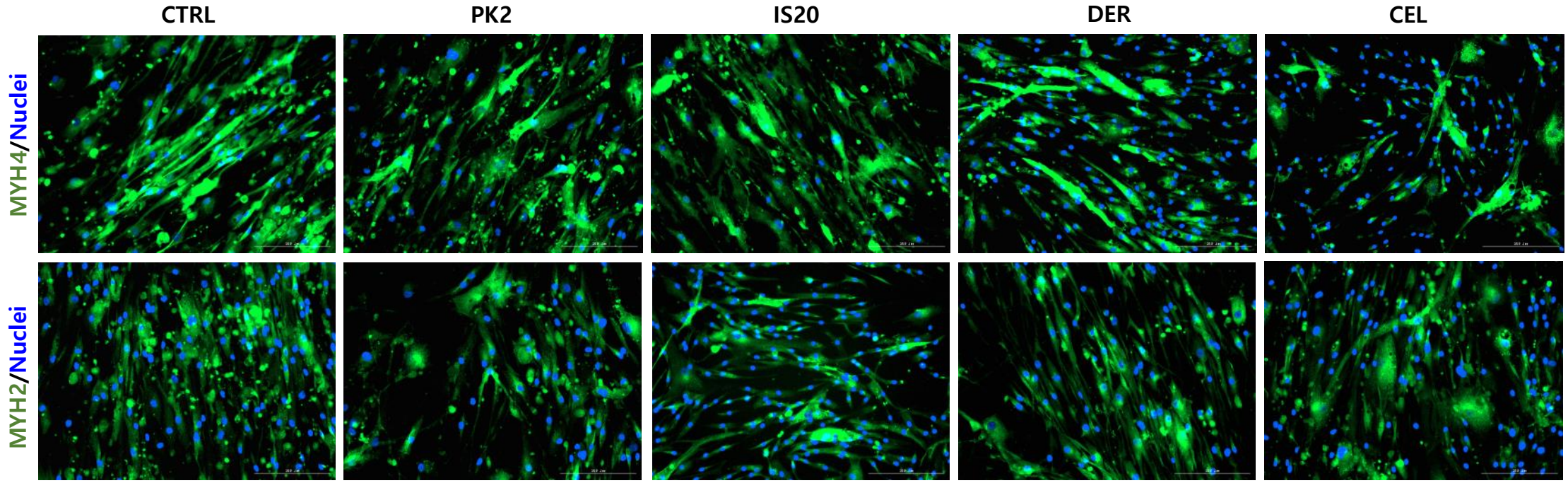

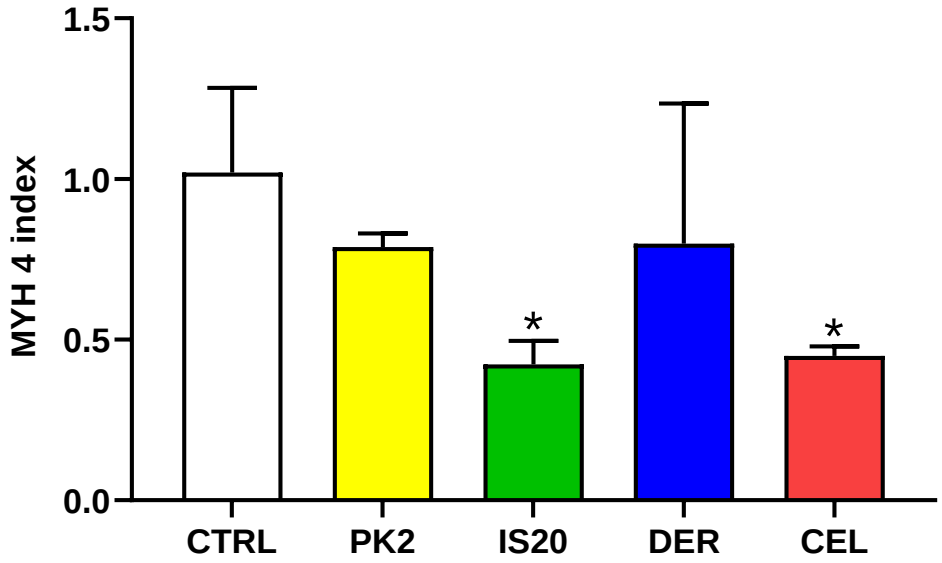

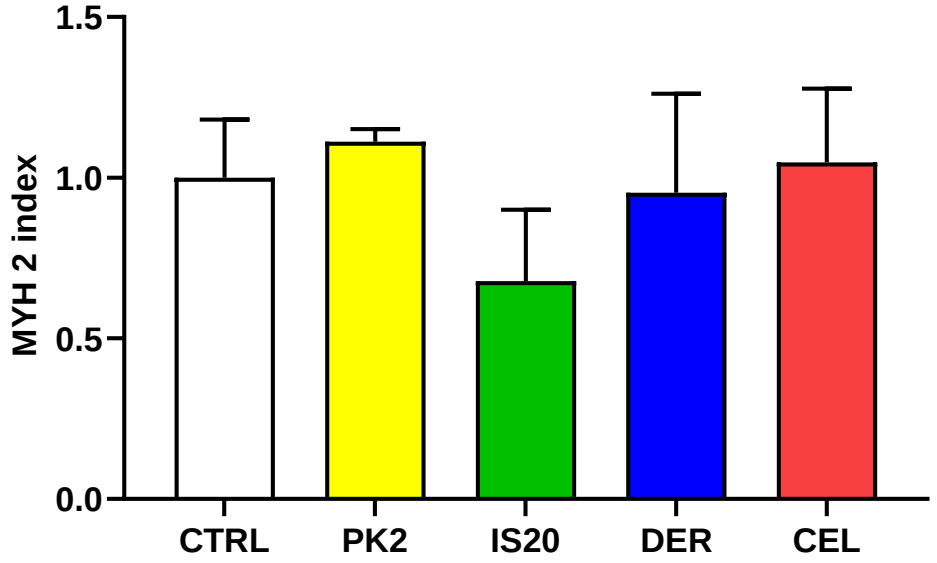

Supplementary Fig. 13

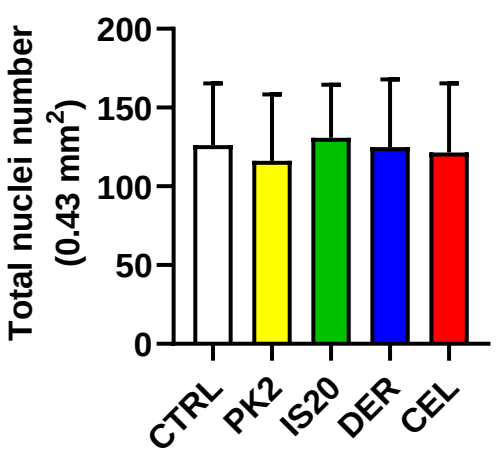

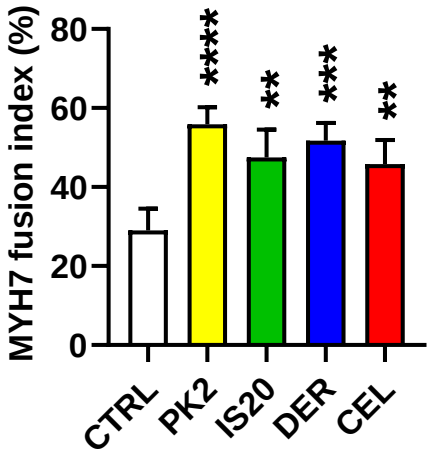

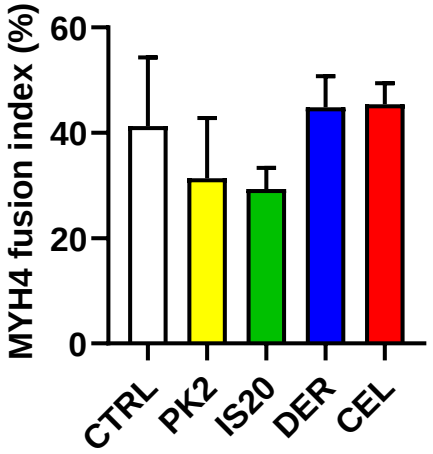

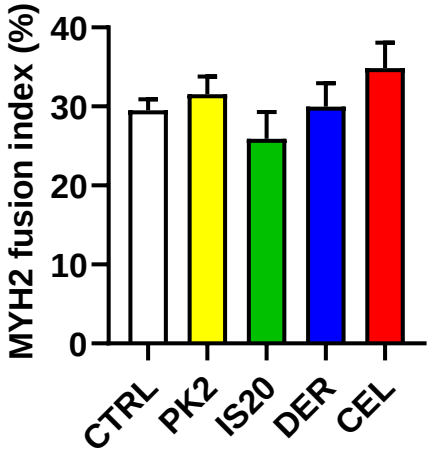

Supplementary Fig. 14

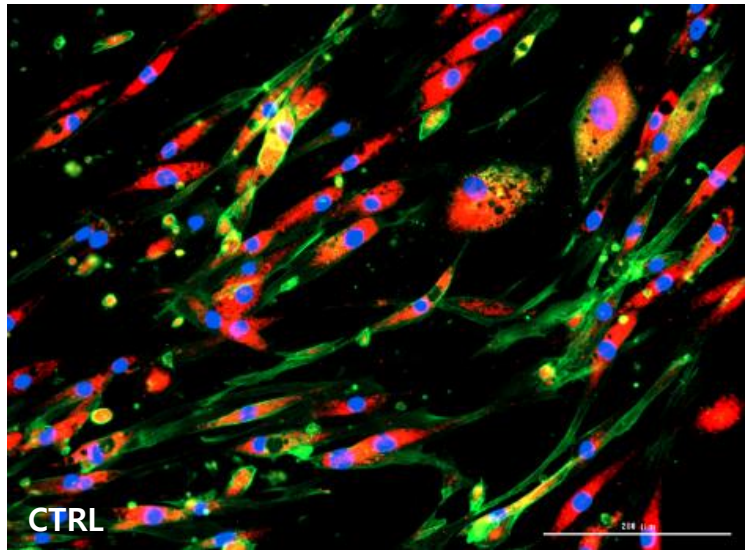

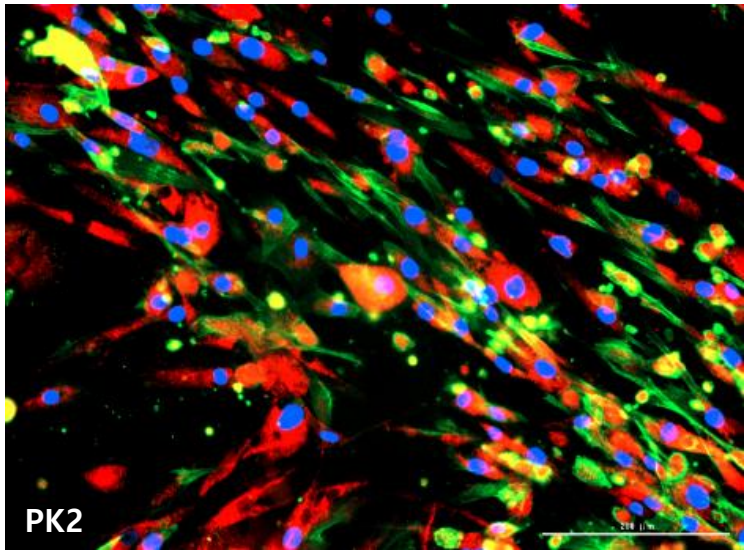

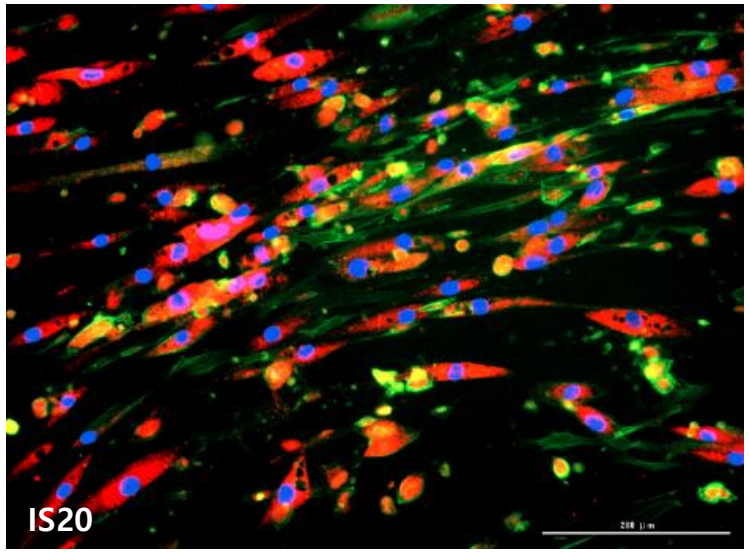

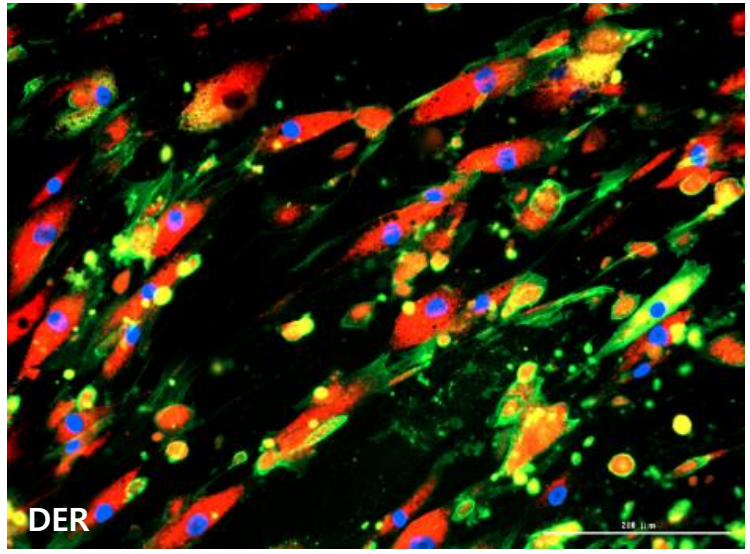

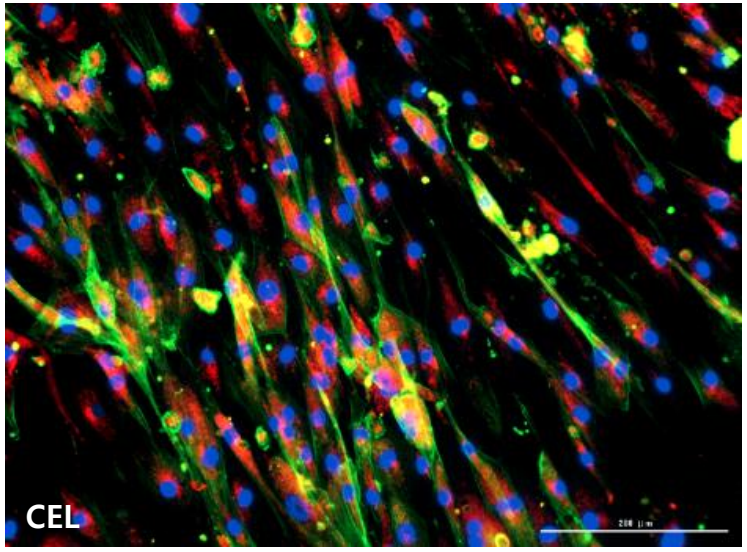

Mitochondria/F-actin/Nuclei

Supplementary Fig. 15

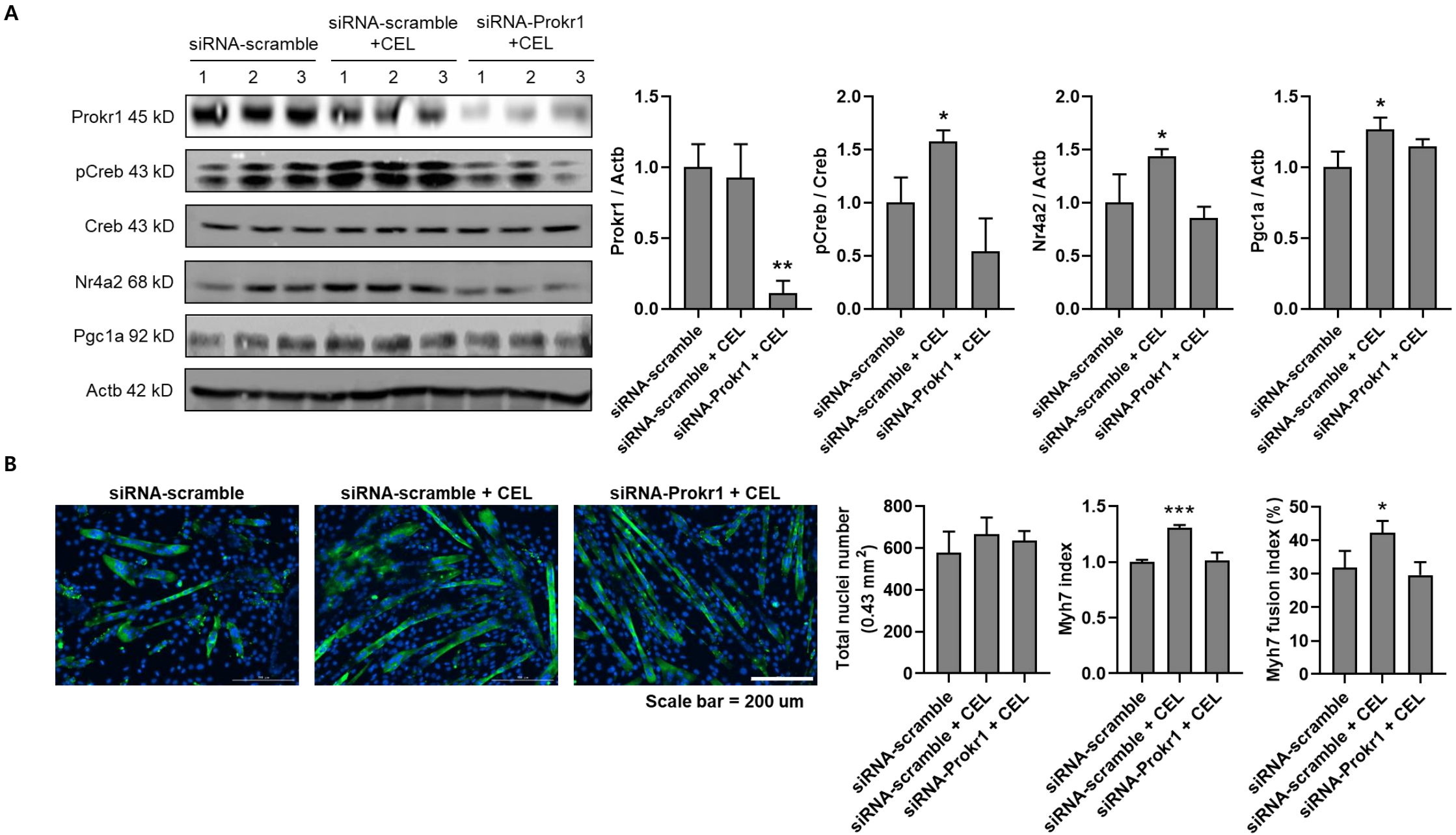

Supplementary Fig. 16

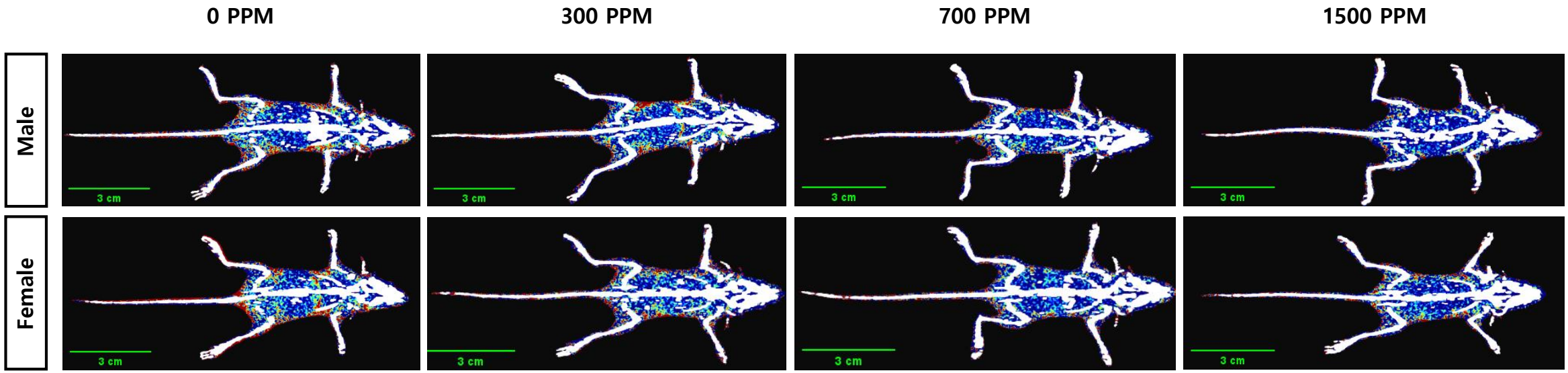

Supplementary Fig. 17

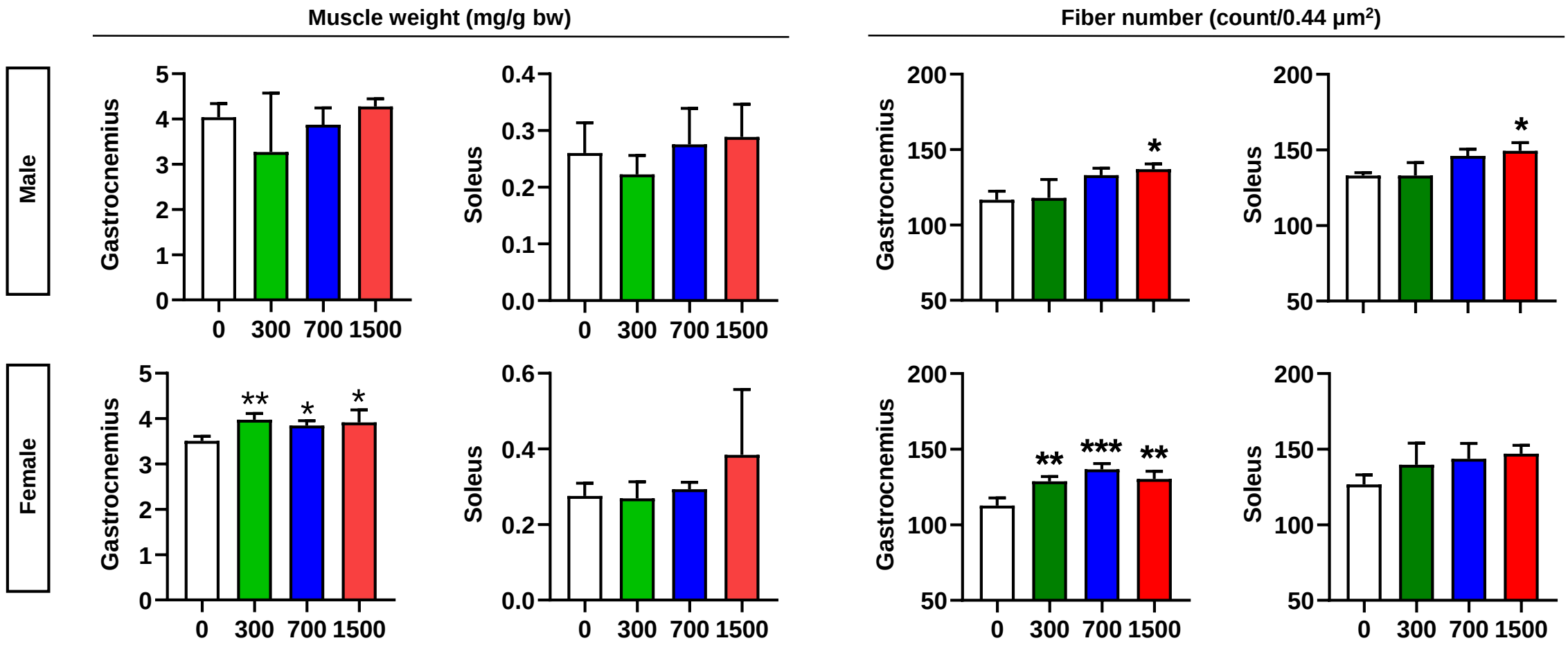

Supplementary Fig. 18

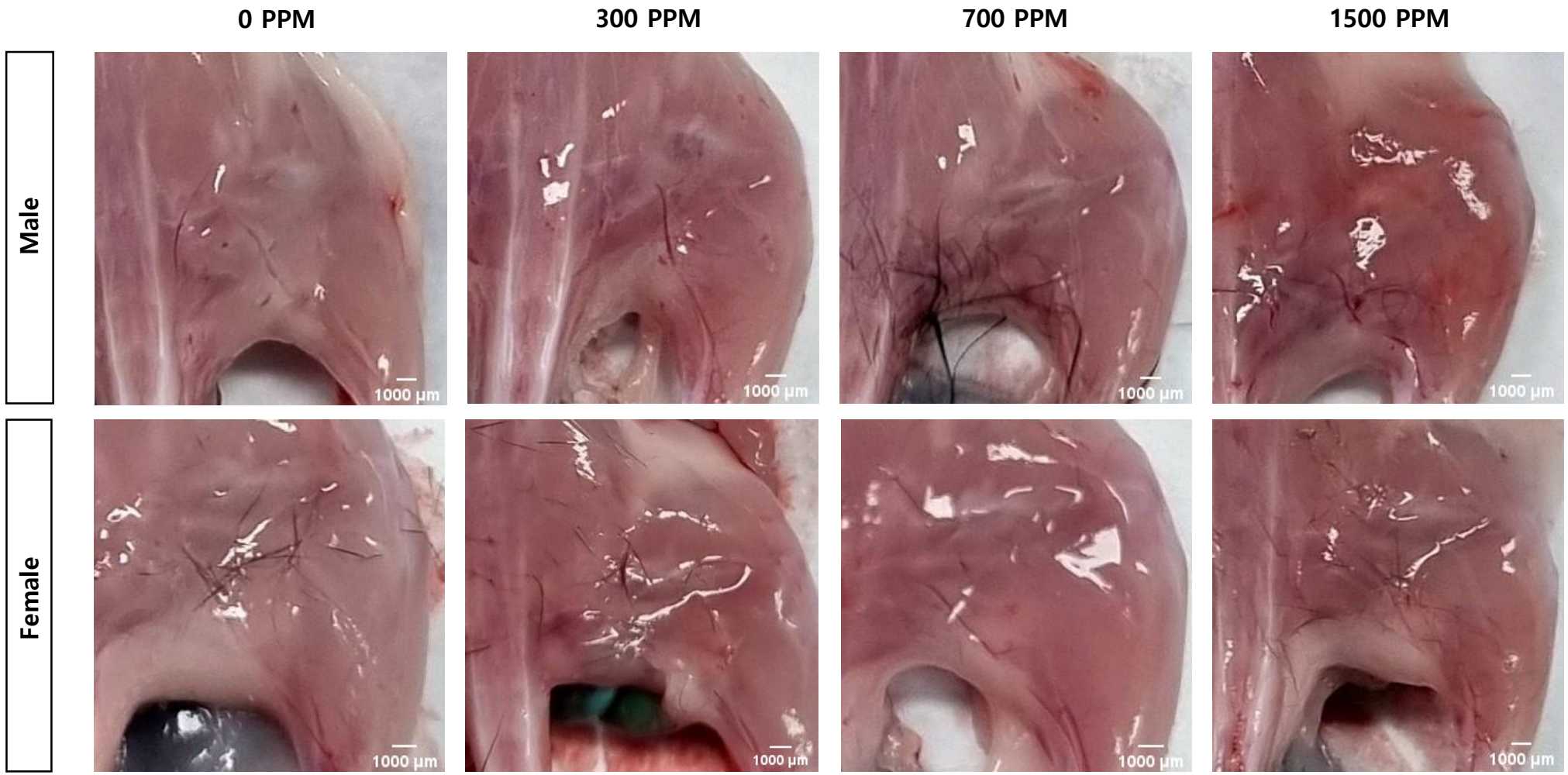

Supplementary Fig. 19

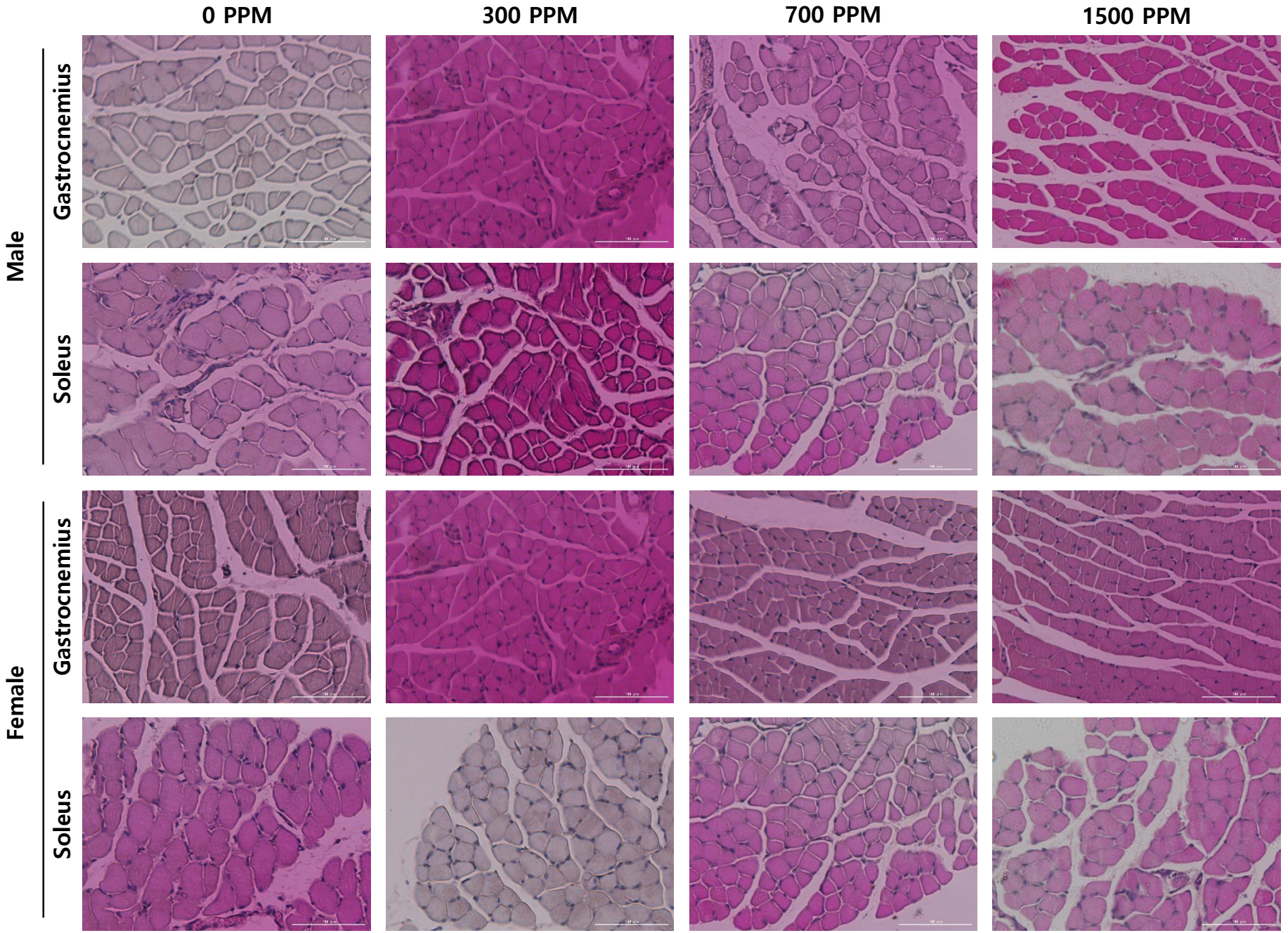

Supplementary Fig. 20

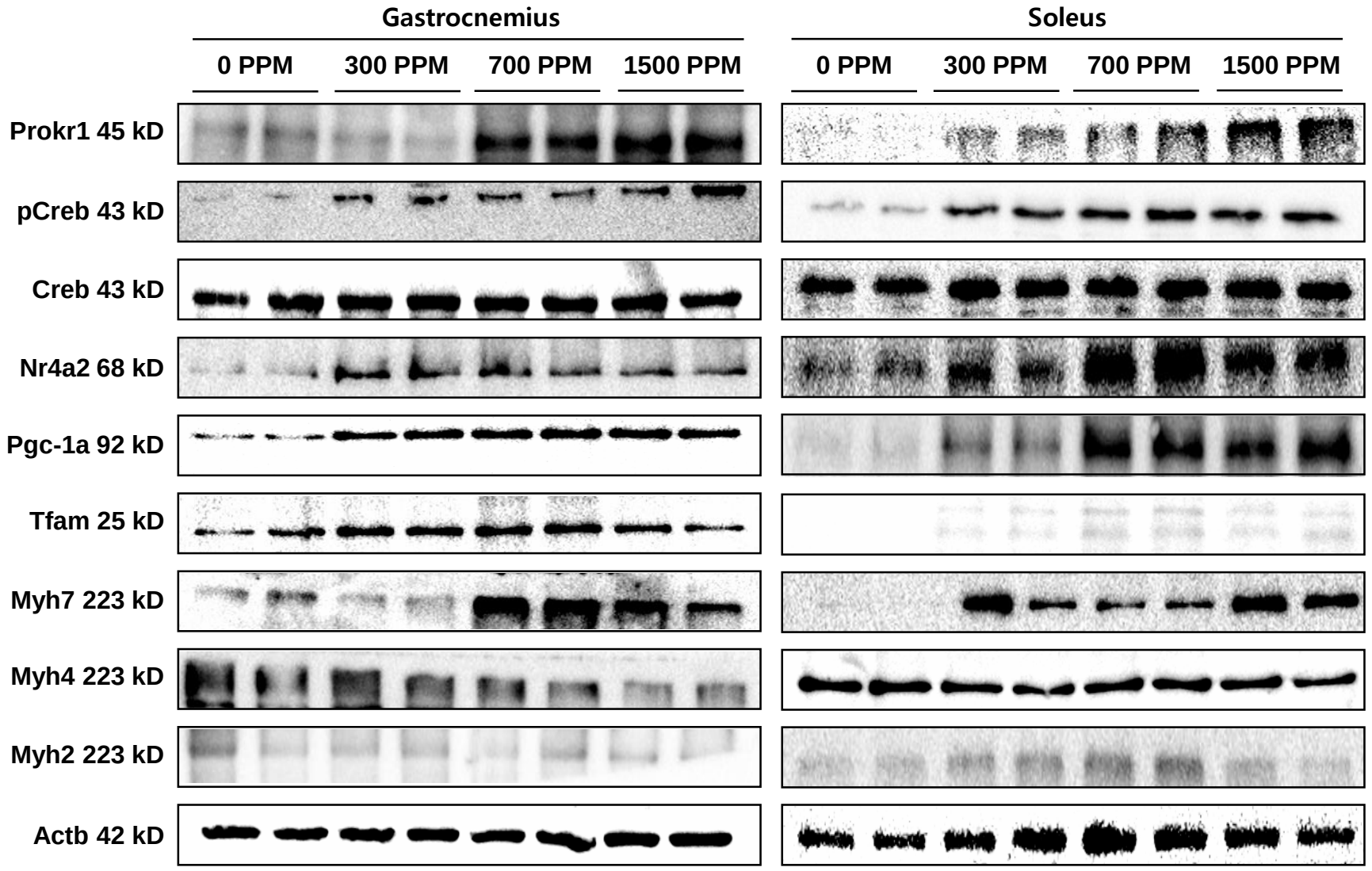

Supplementary Fig. 21

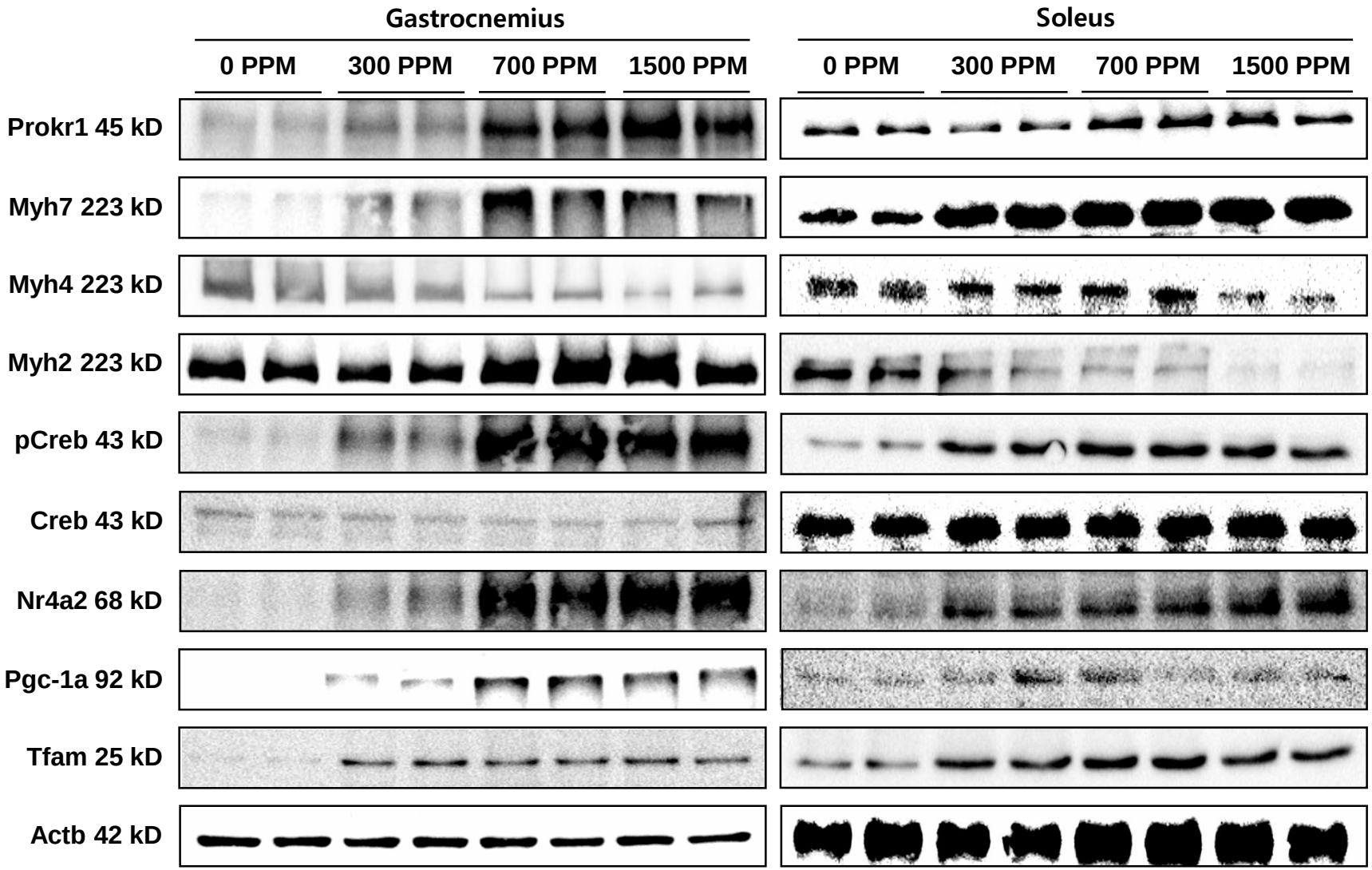

Supplementary Fig. 22

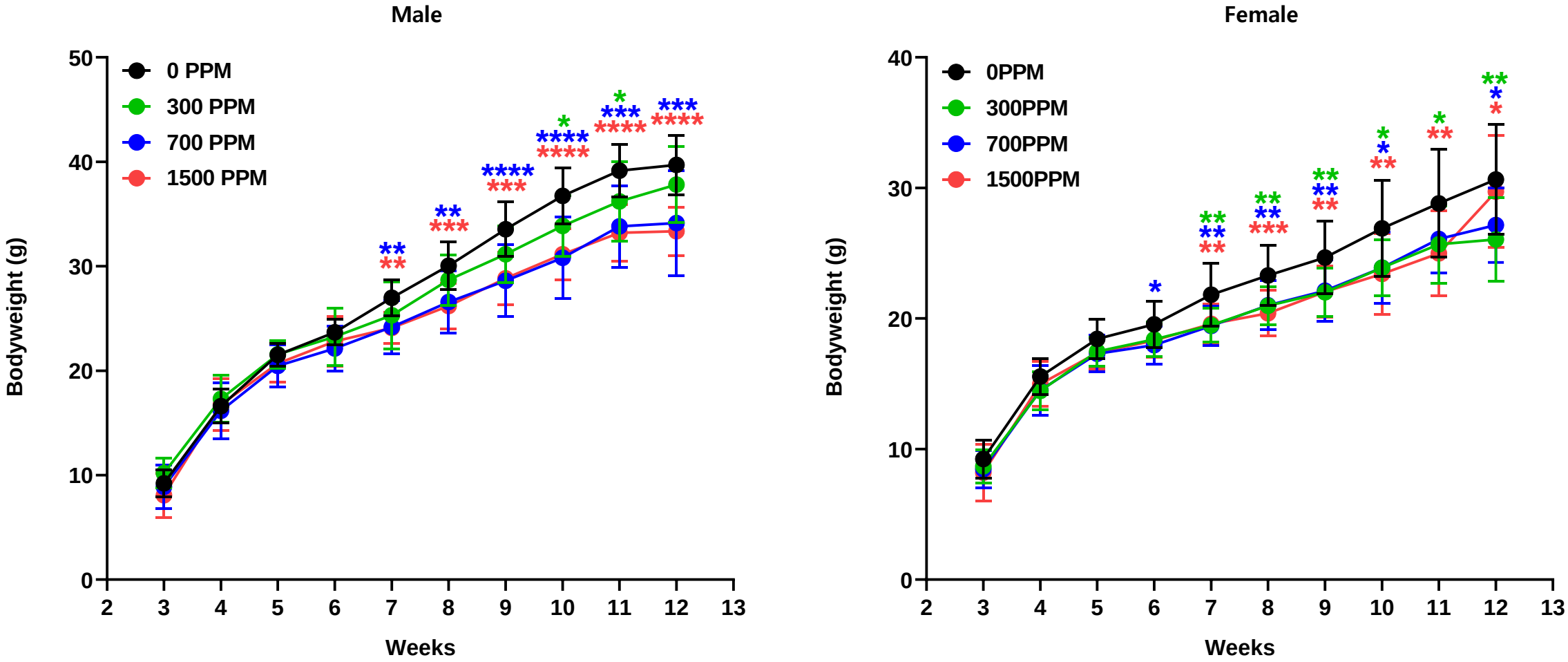

Supplementary Fig. 23

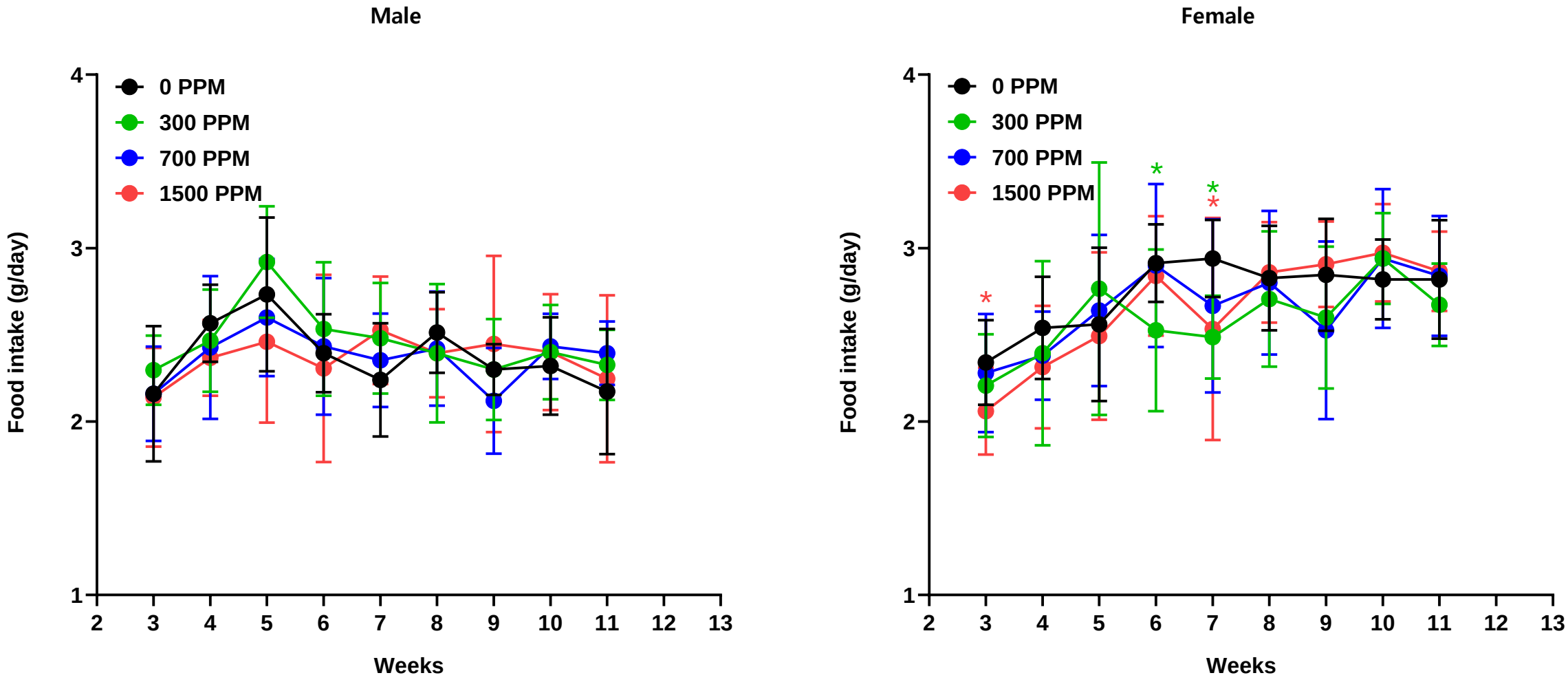

Supplementary Fig. 24

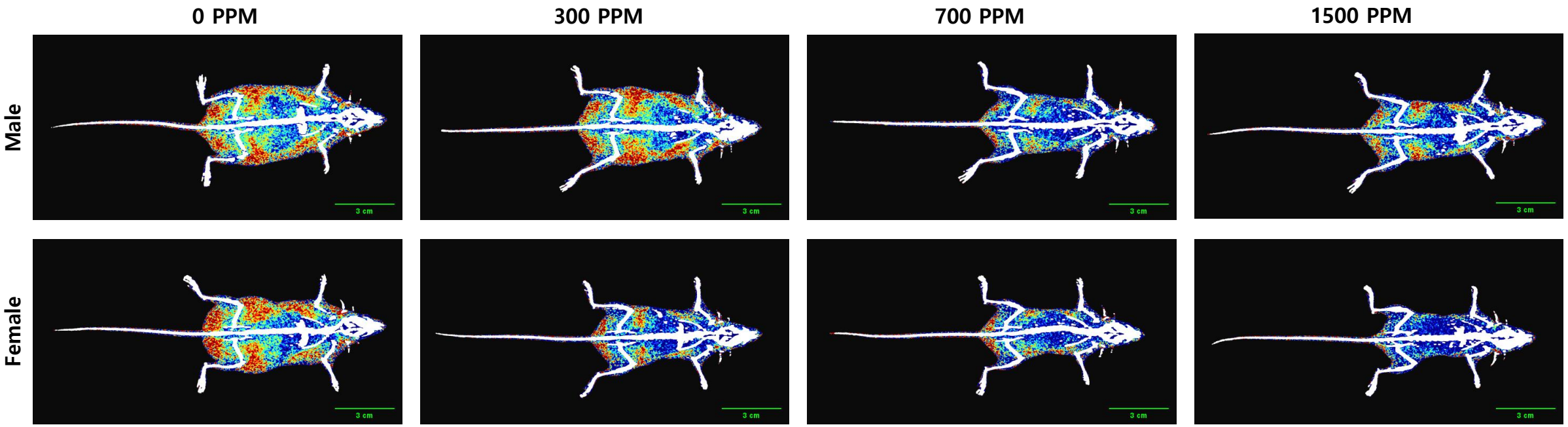

Supplementary Fig. 25

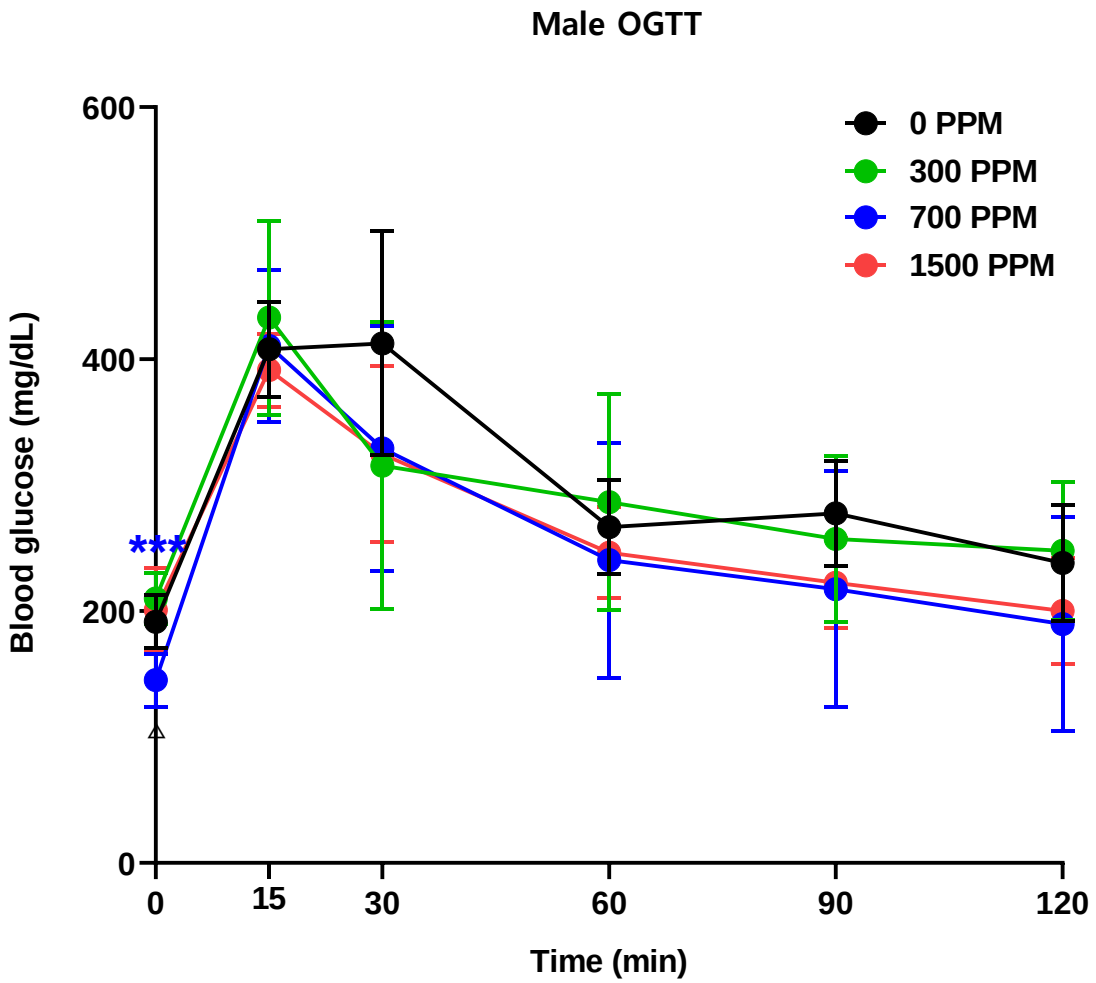

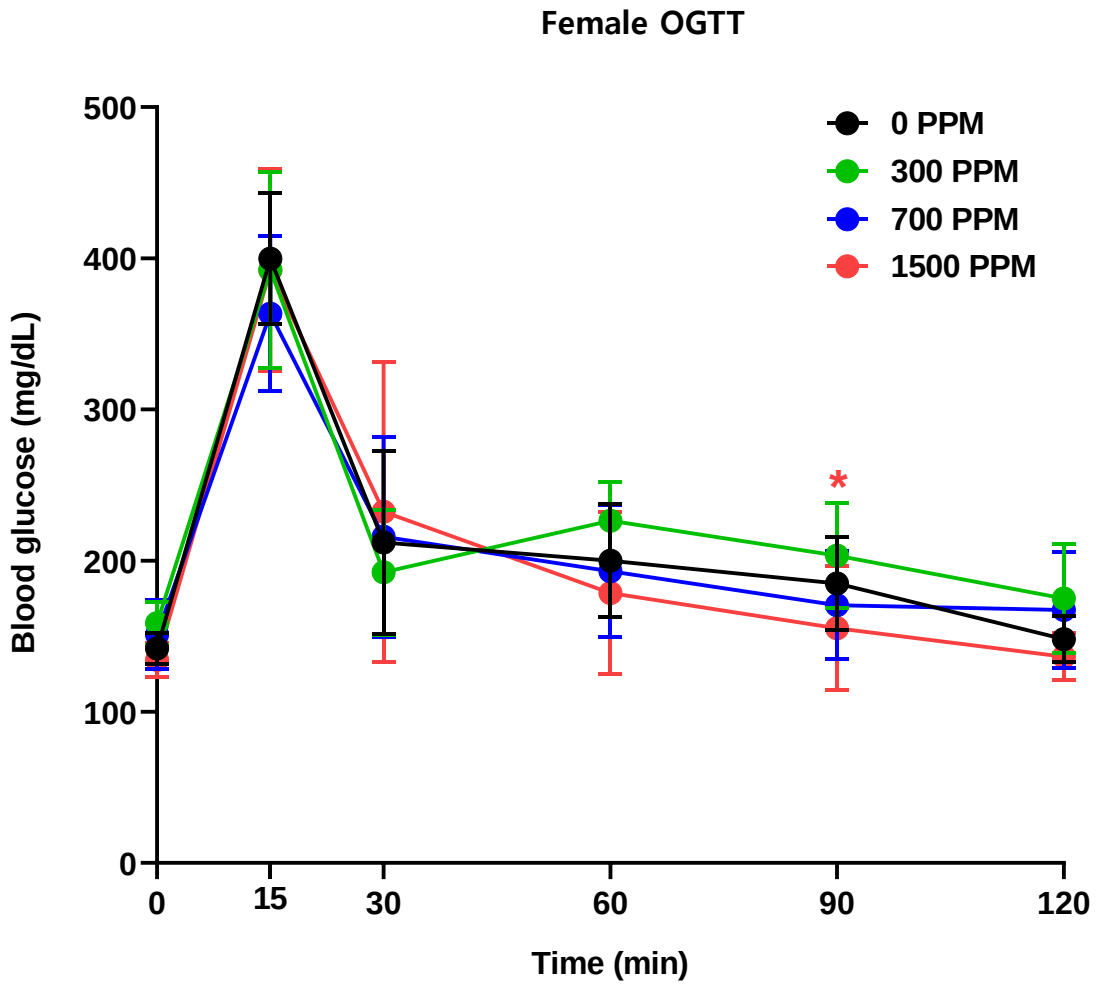

Supplementary Fig. 26

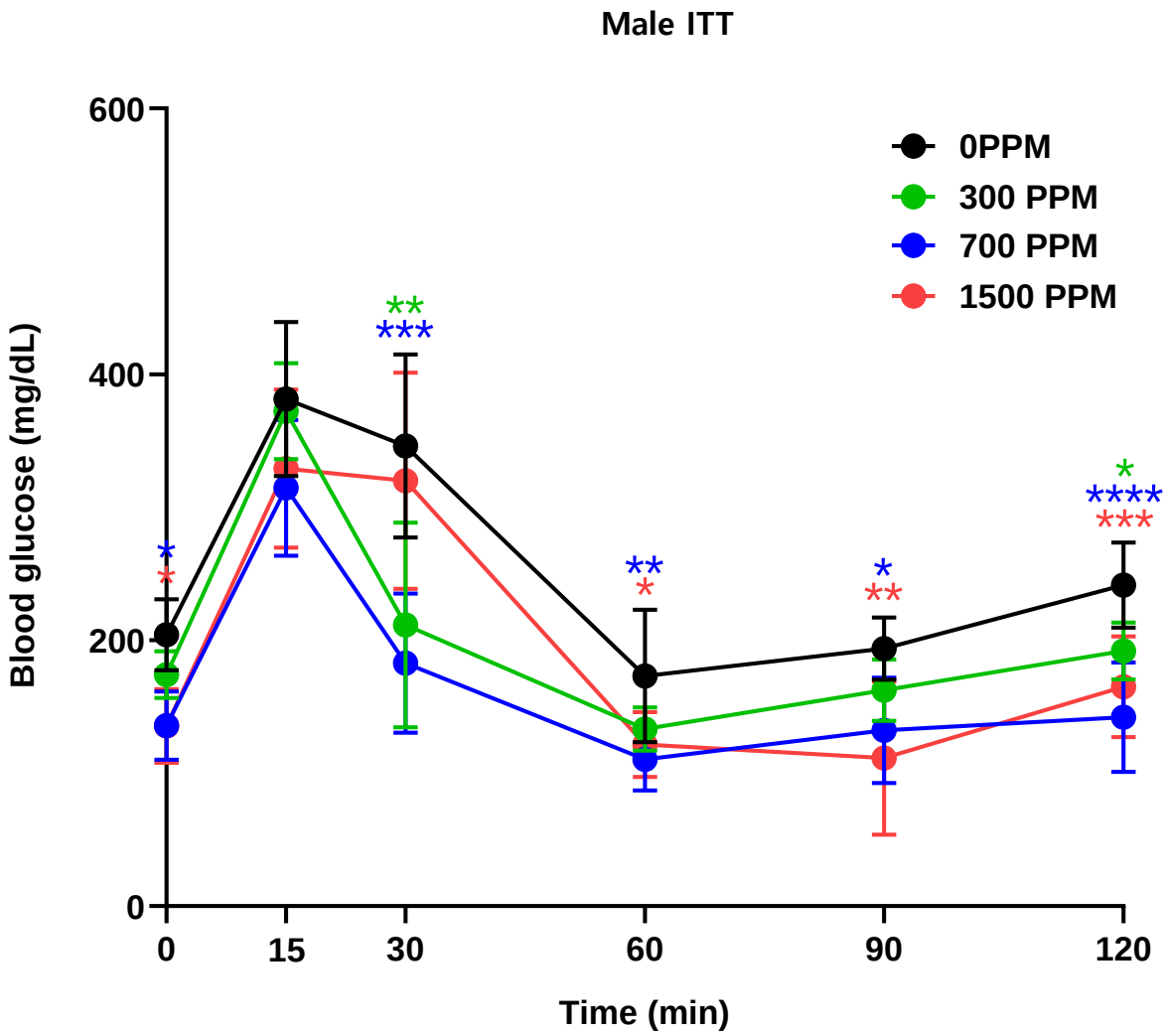

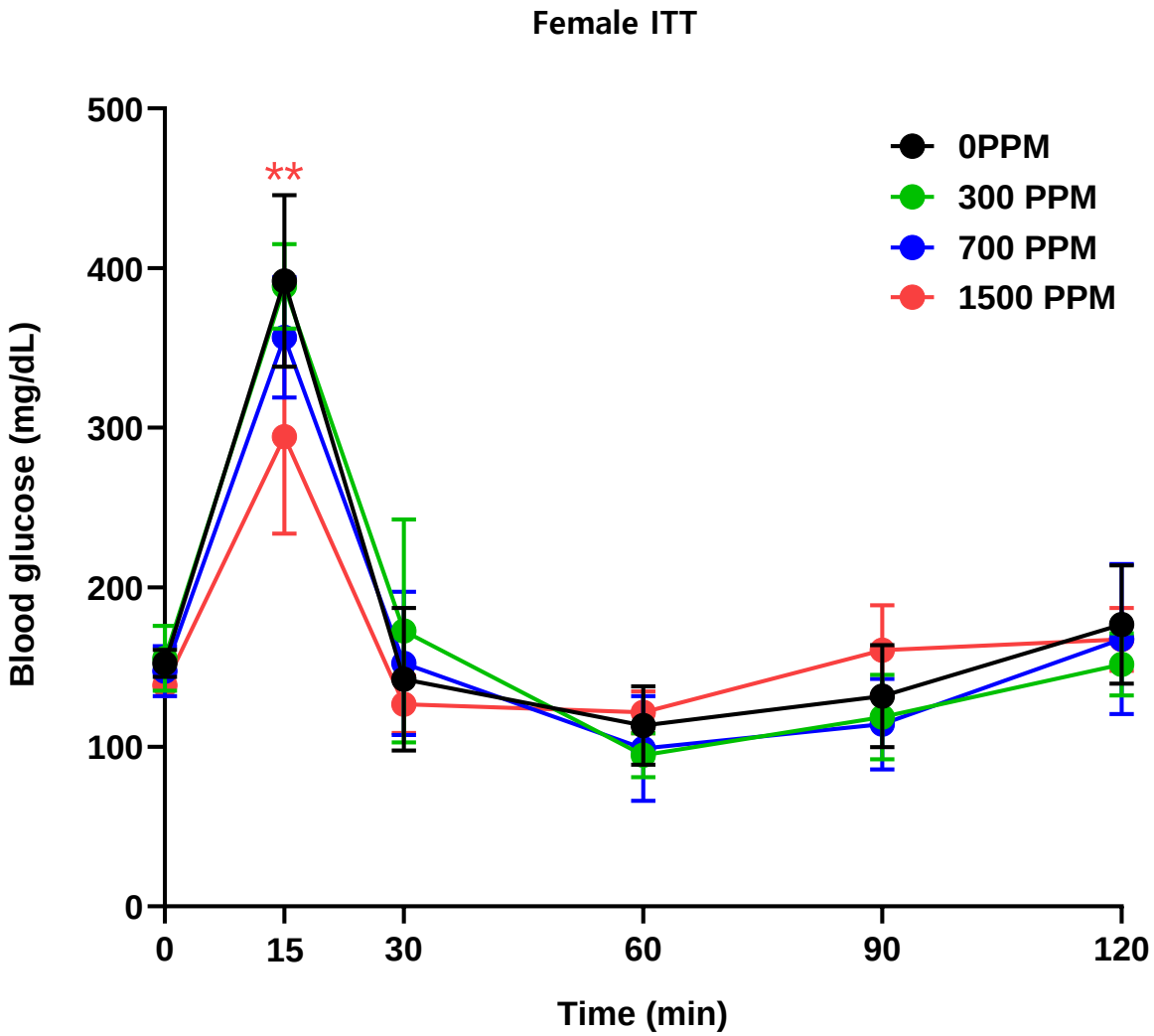

Supplementary Fig. 27

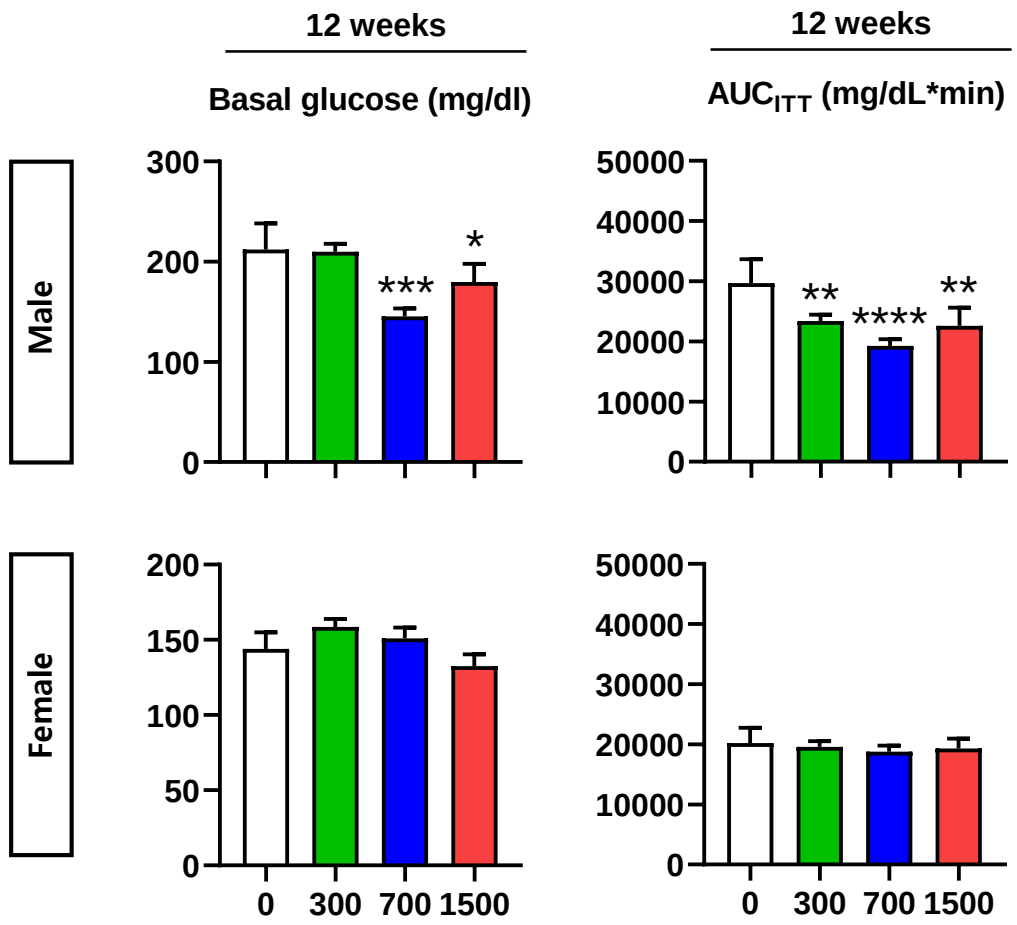

Supplementary Fig. 28

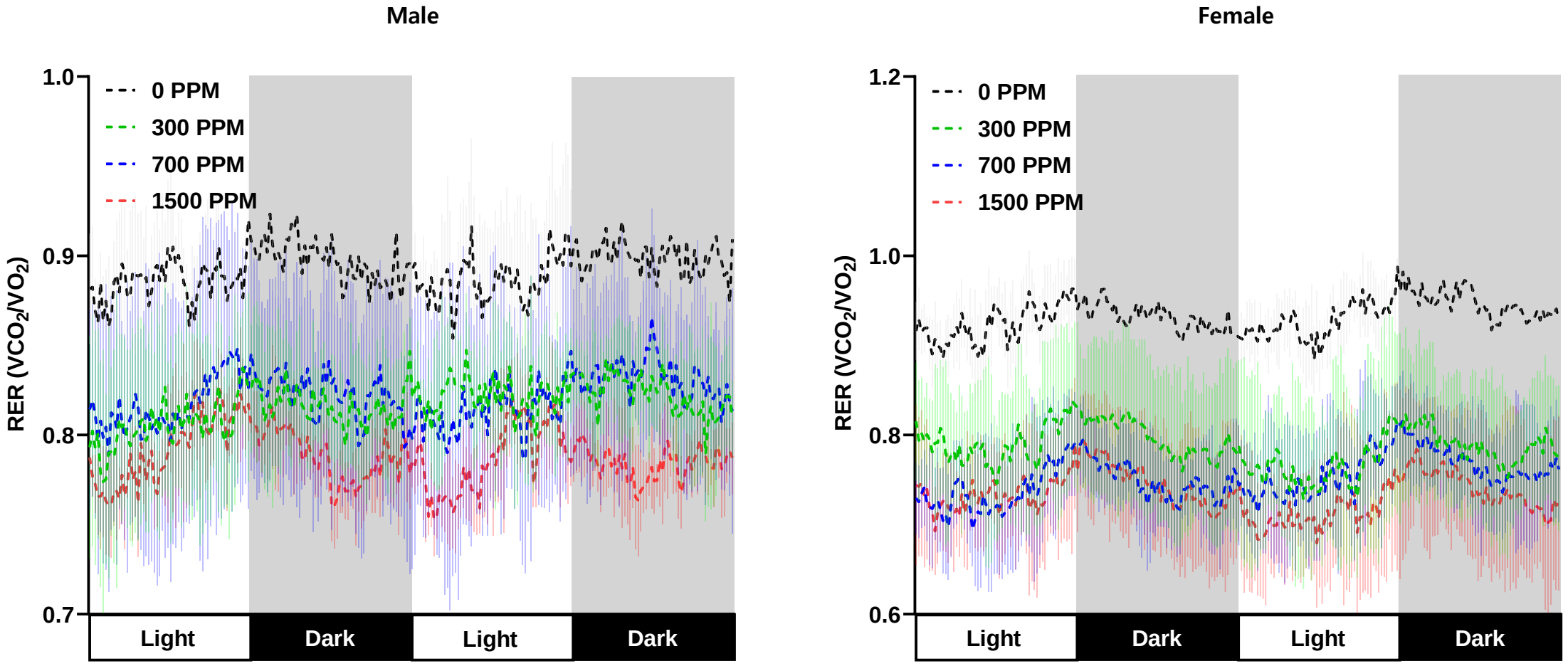

Supplementary Fig. 29

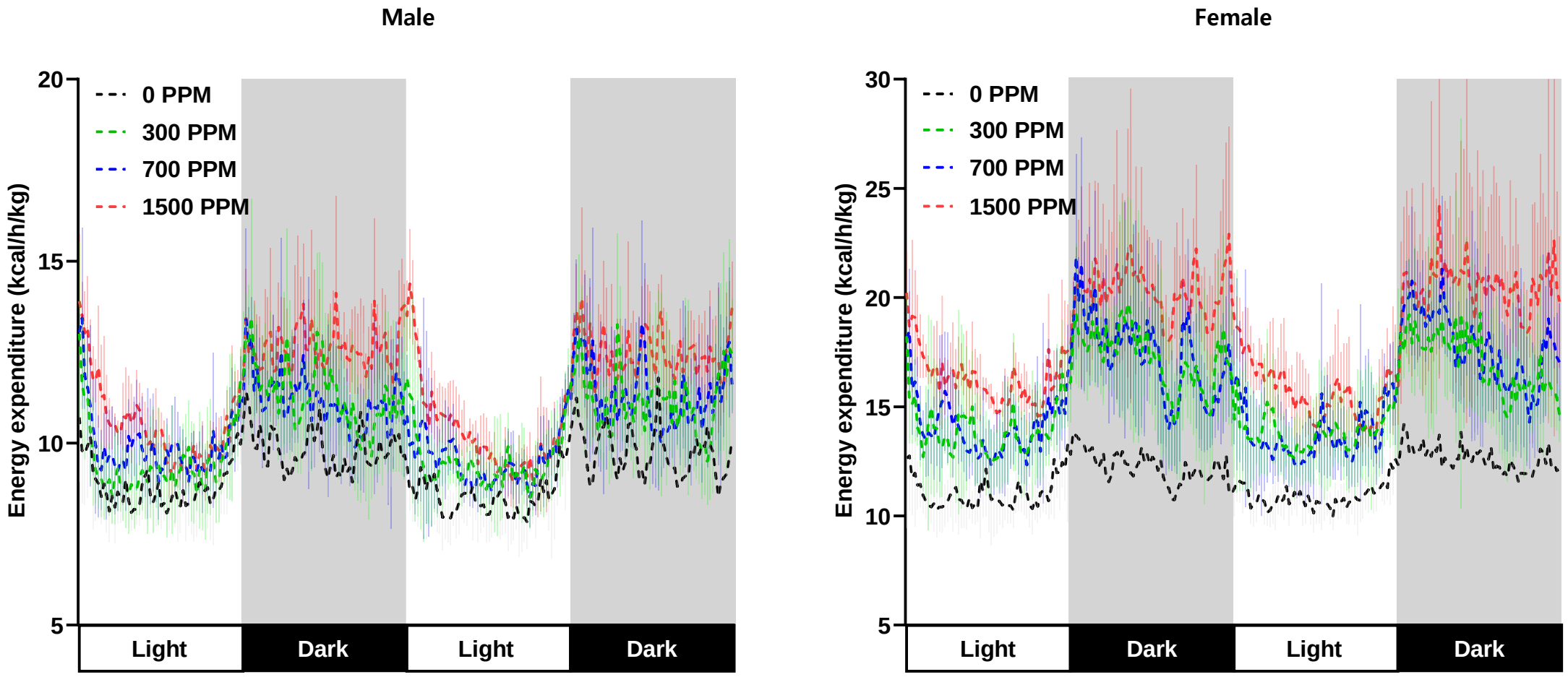

Supplementary Fig. 30

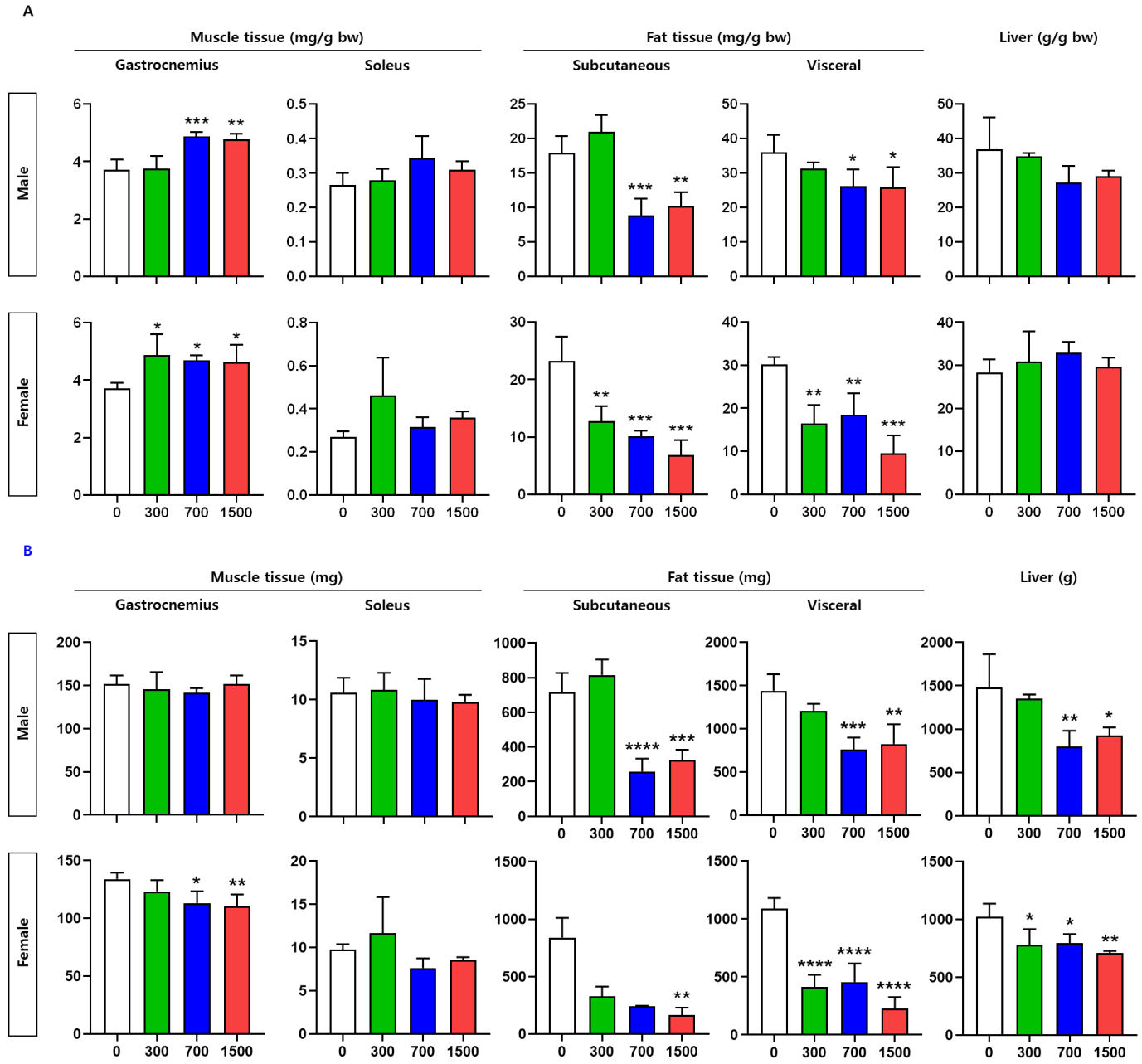

Supplementary Fig. 31

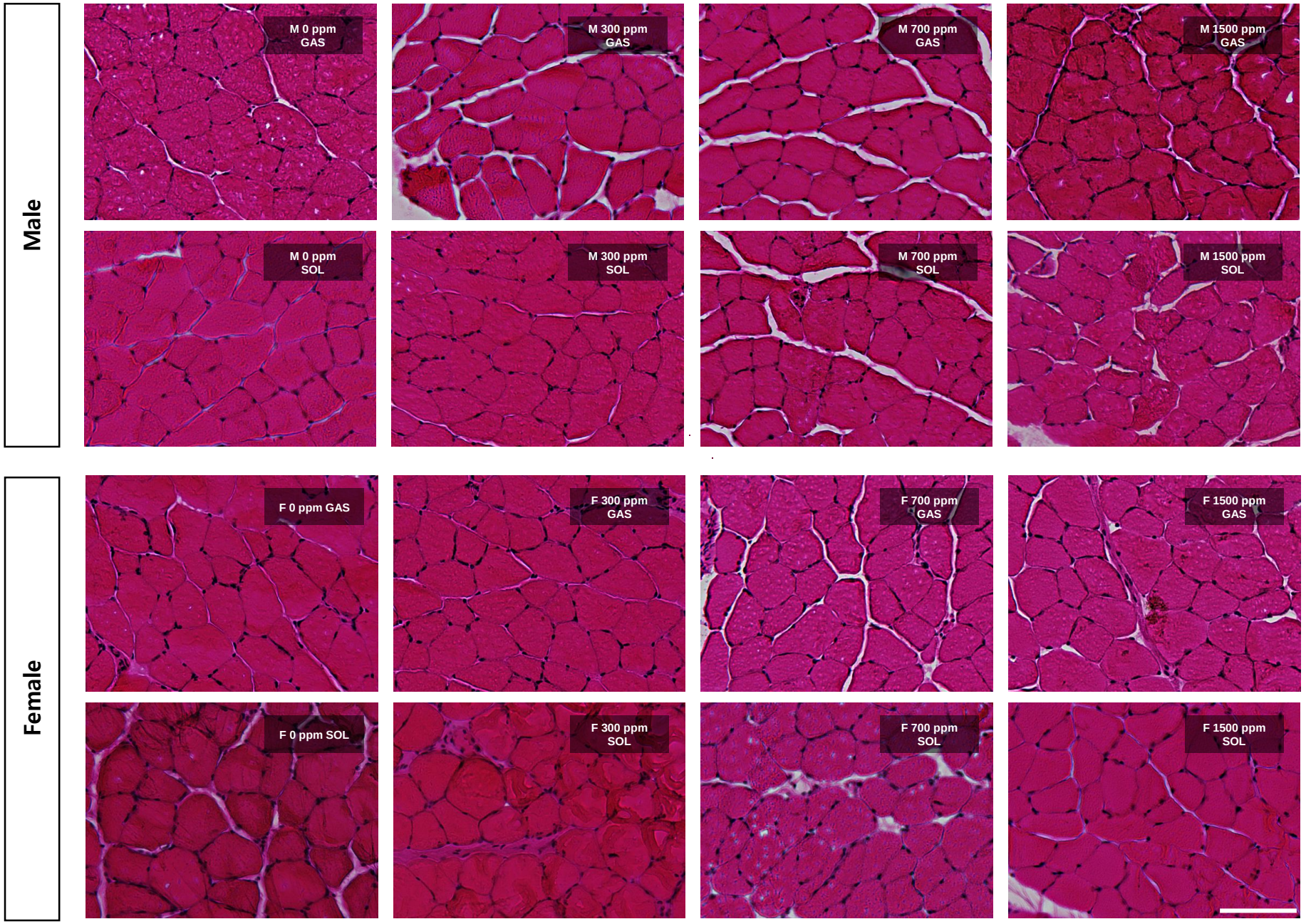

Supplementary Fig. 32

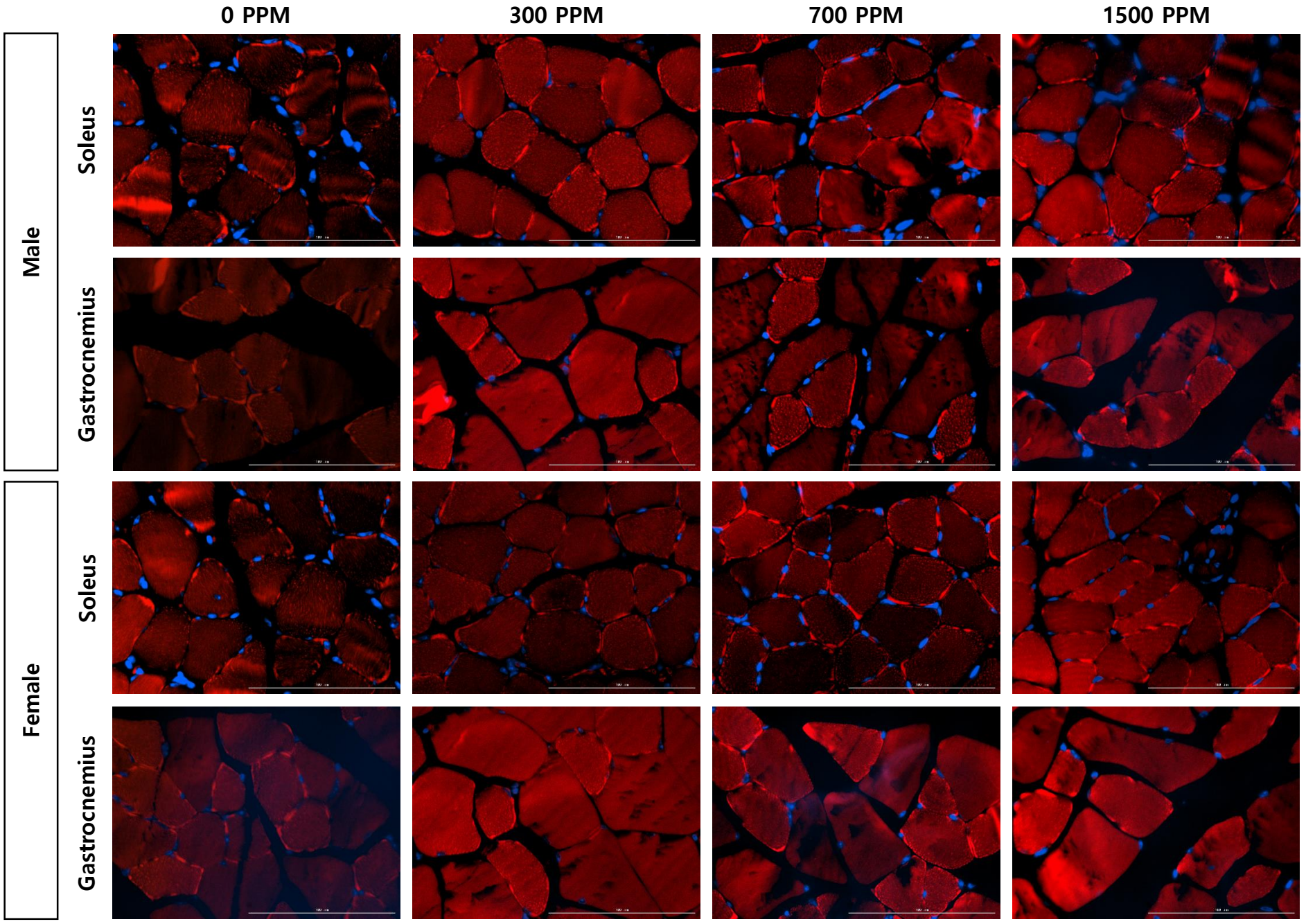

Supplementary Fig. 33

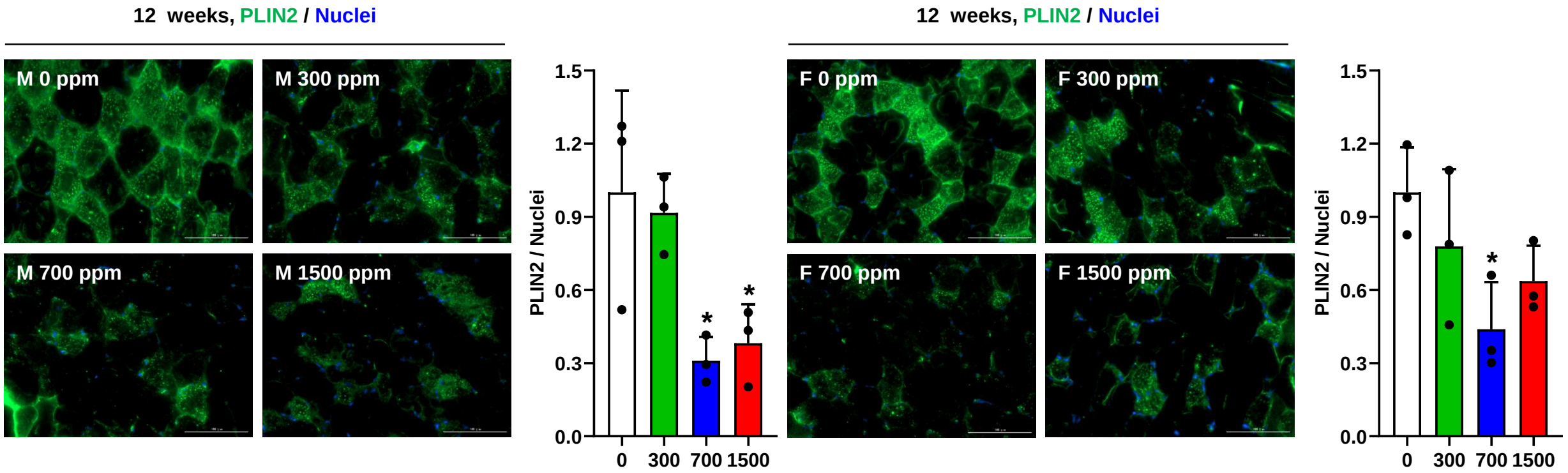

Supplementary Fig. 34

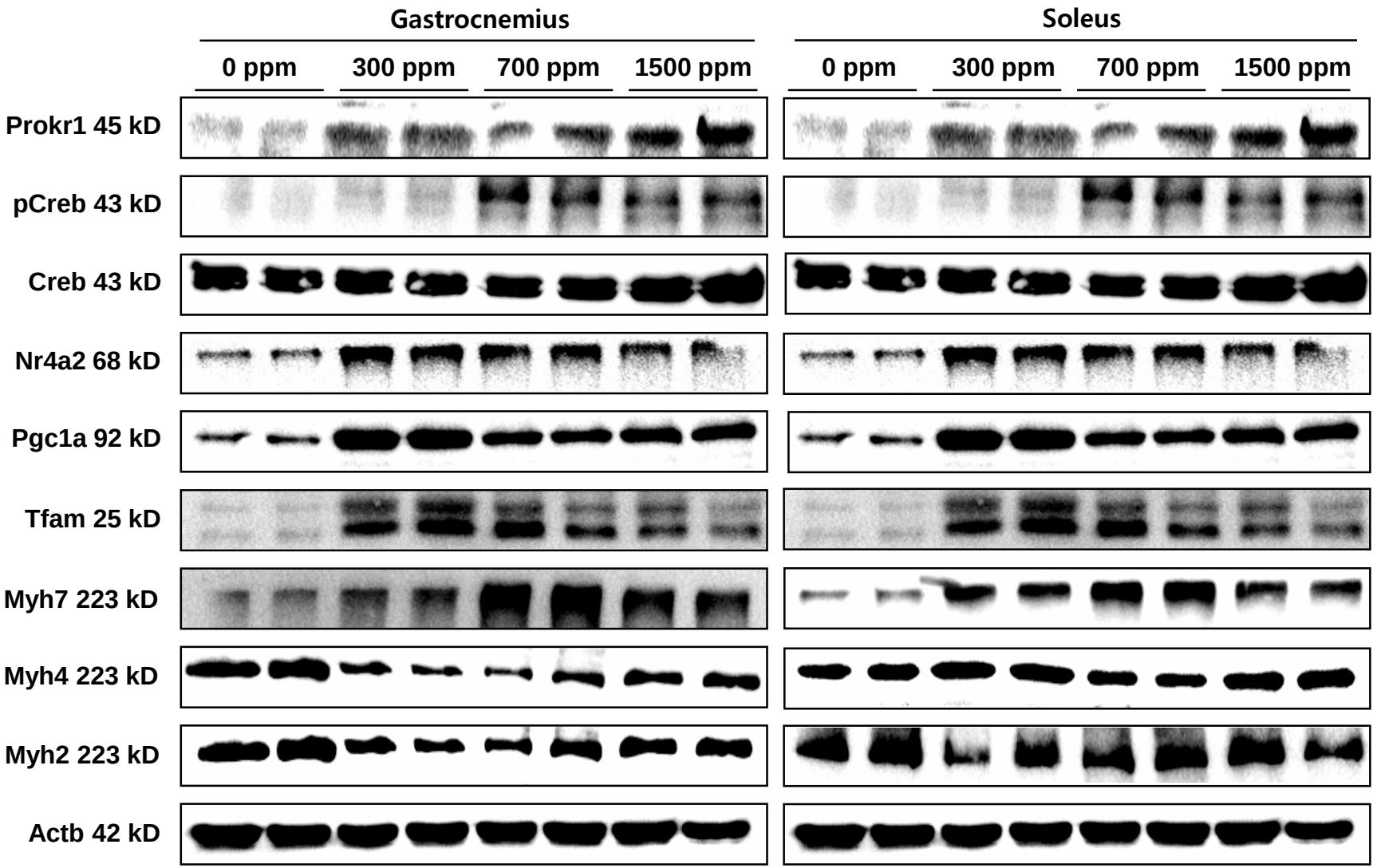

Supplementary Fig. 35

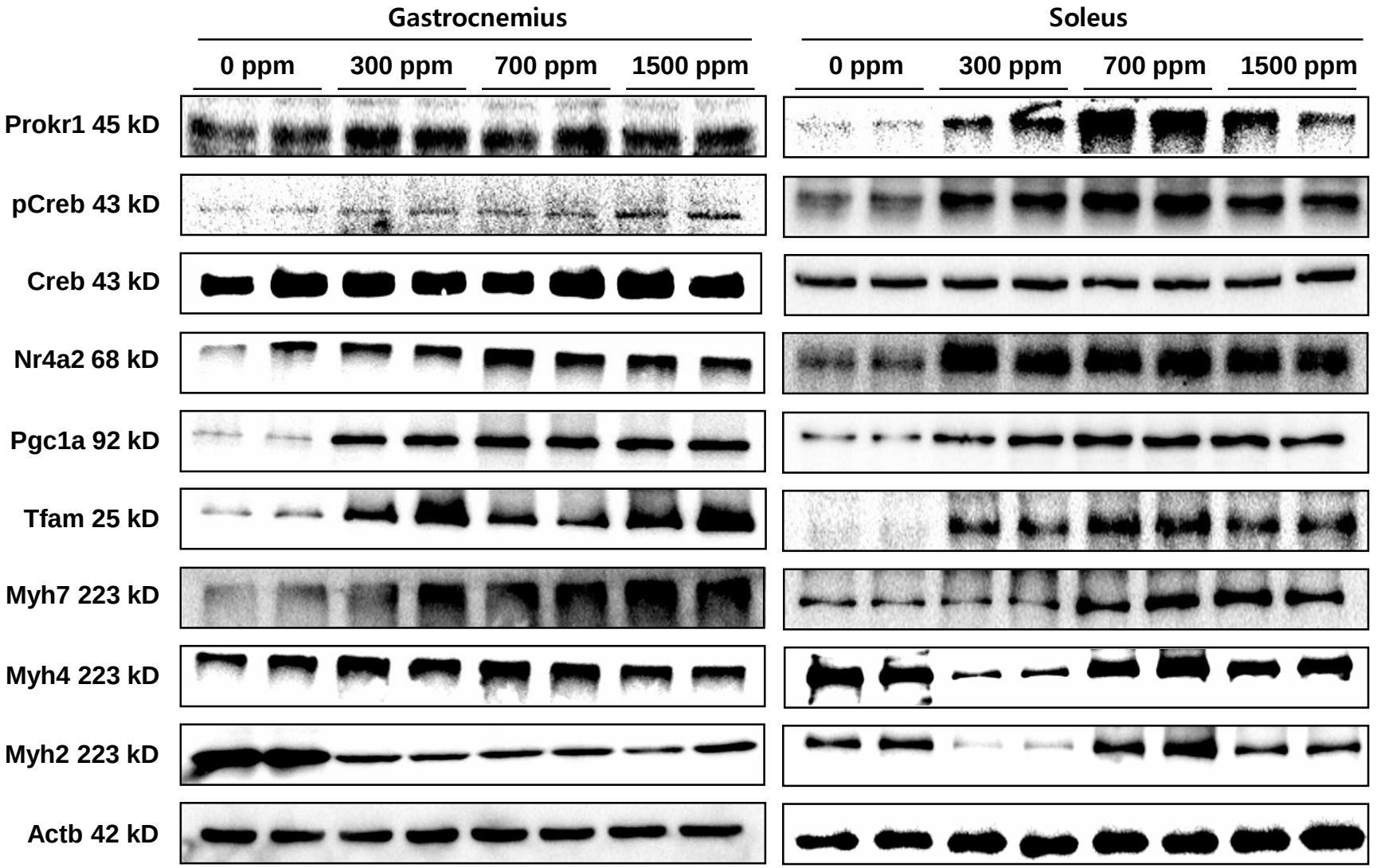

Supplementary Fig. 36

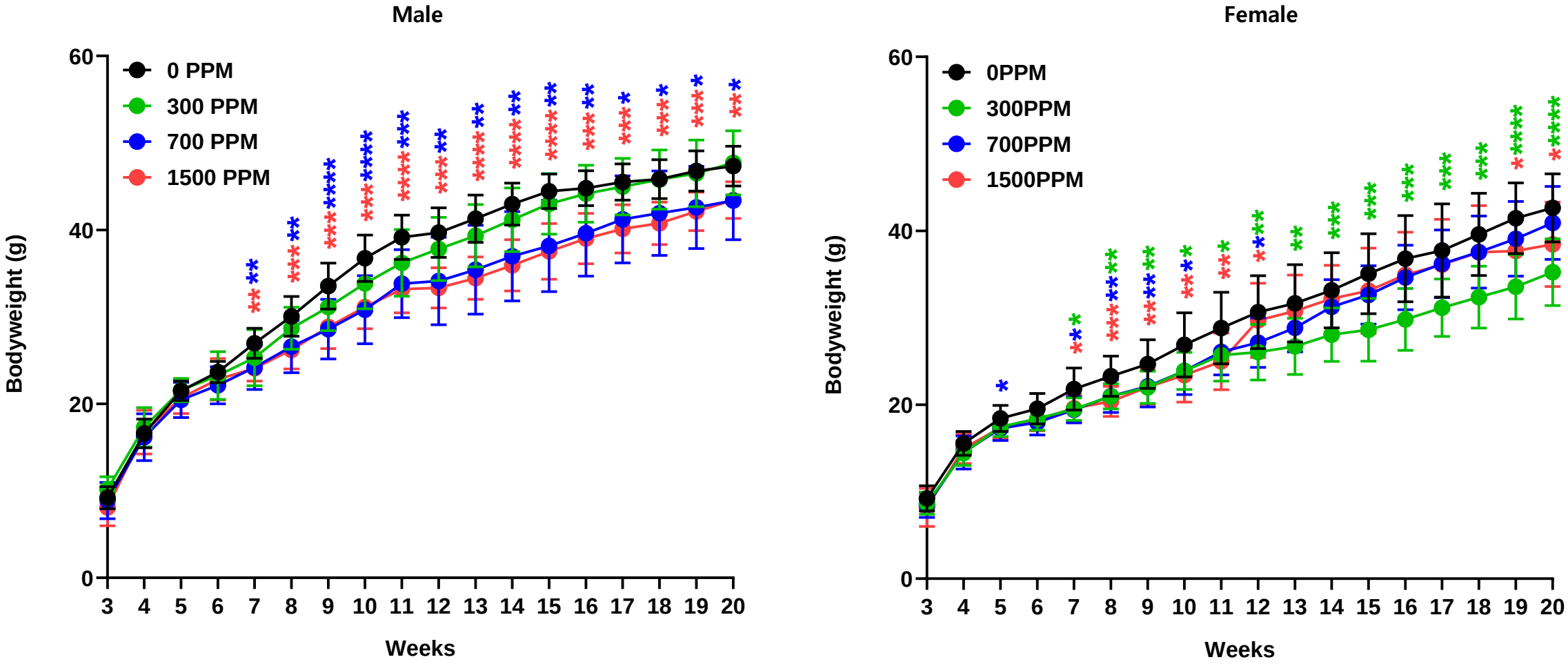

Supplementary Fig. 37

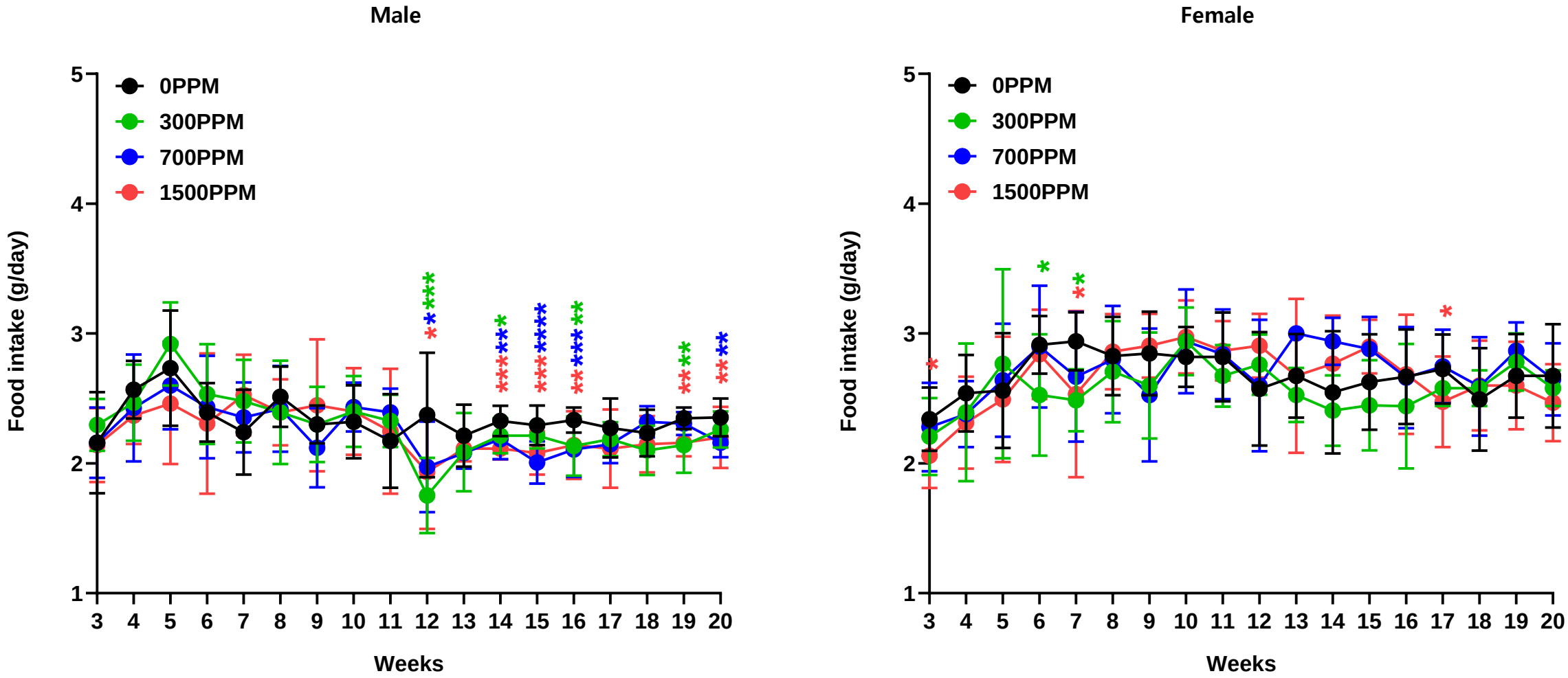

Supplementary Fig. 38

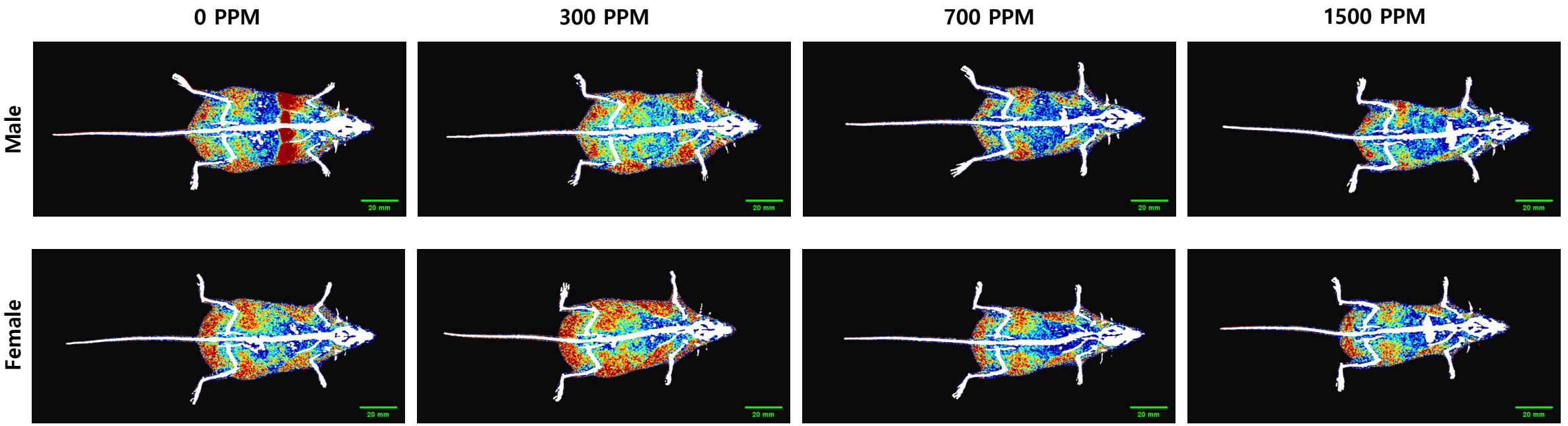

Supplementary Fig. 39

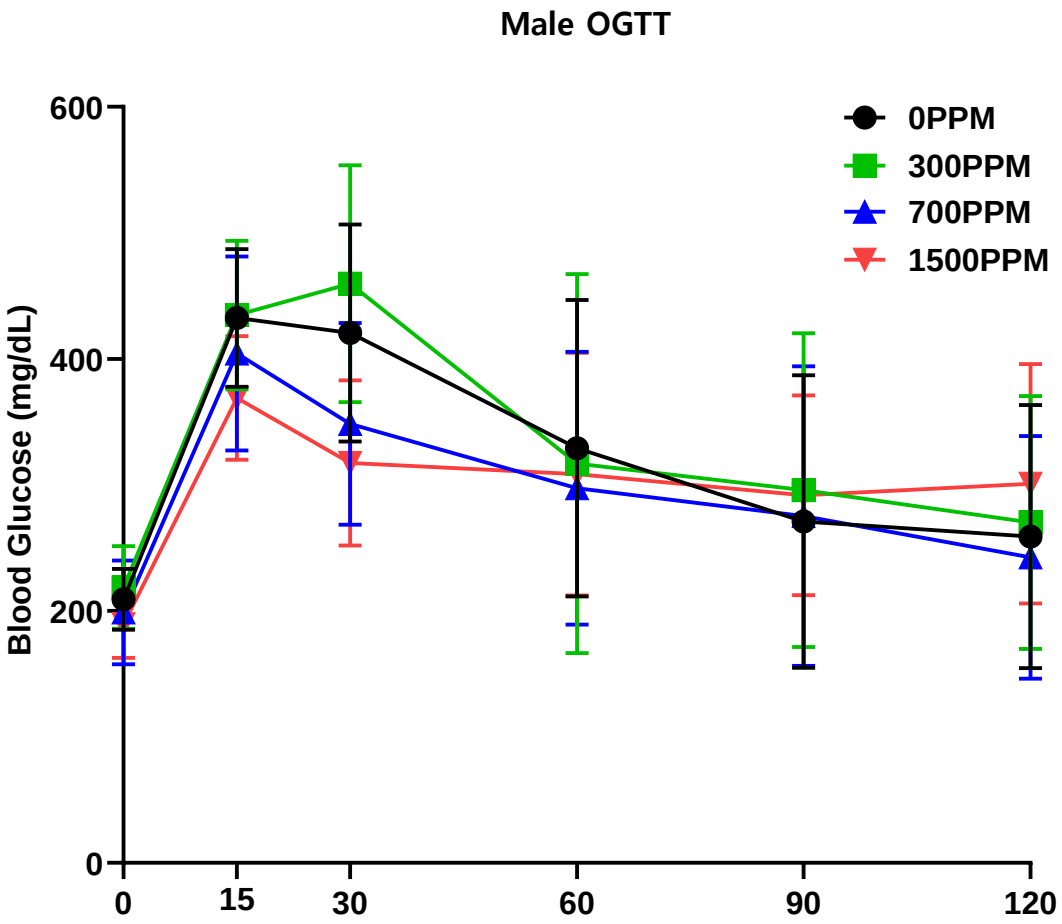

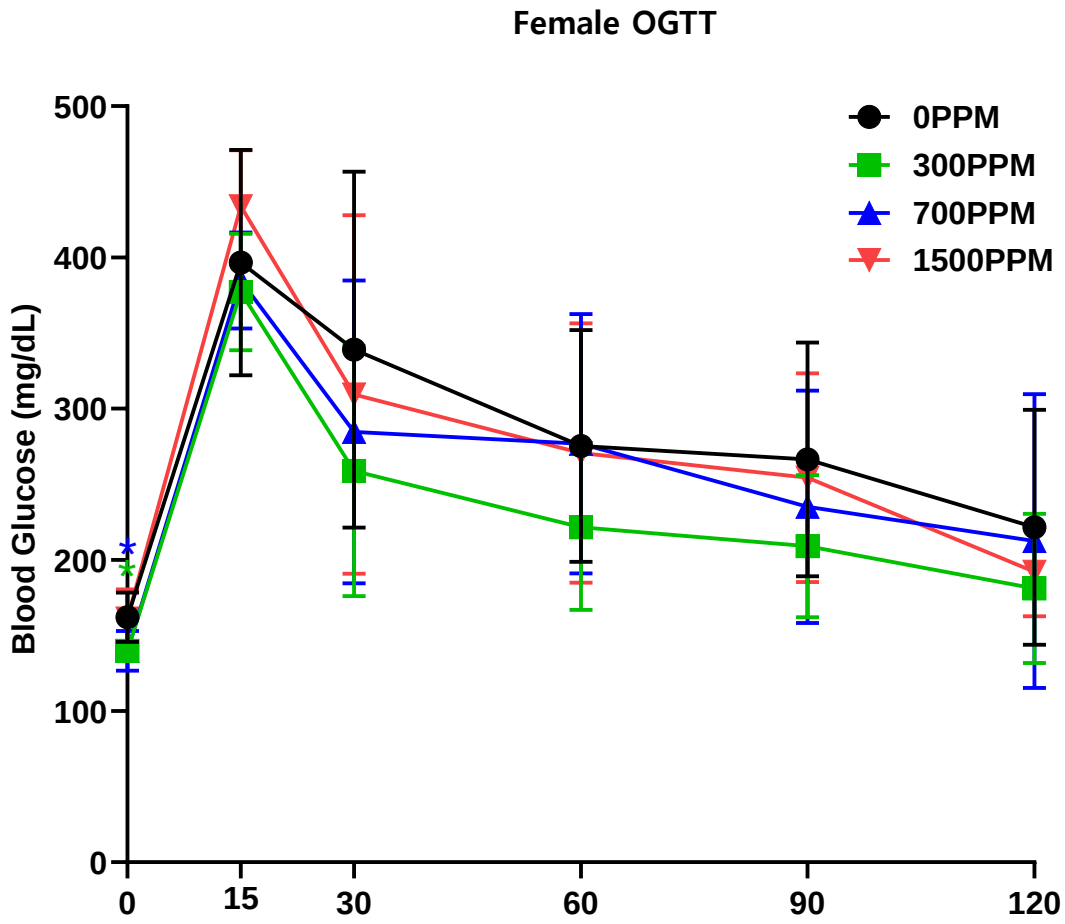

Supplementary Fig. 40

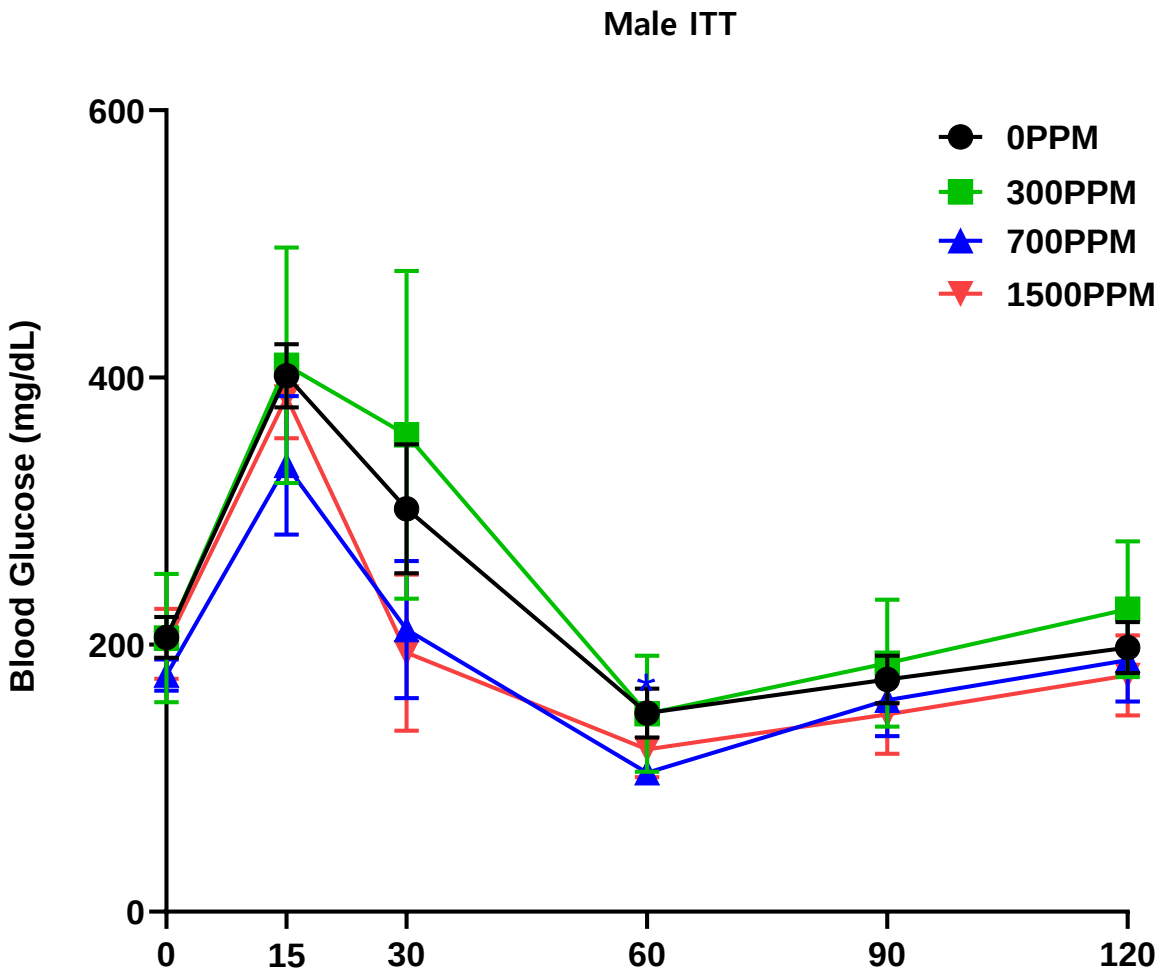

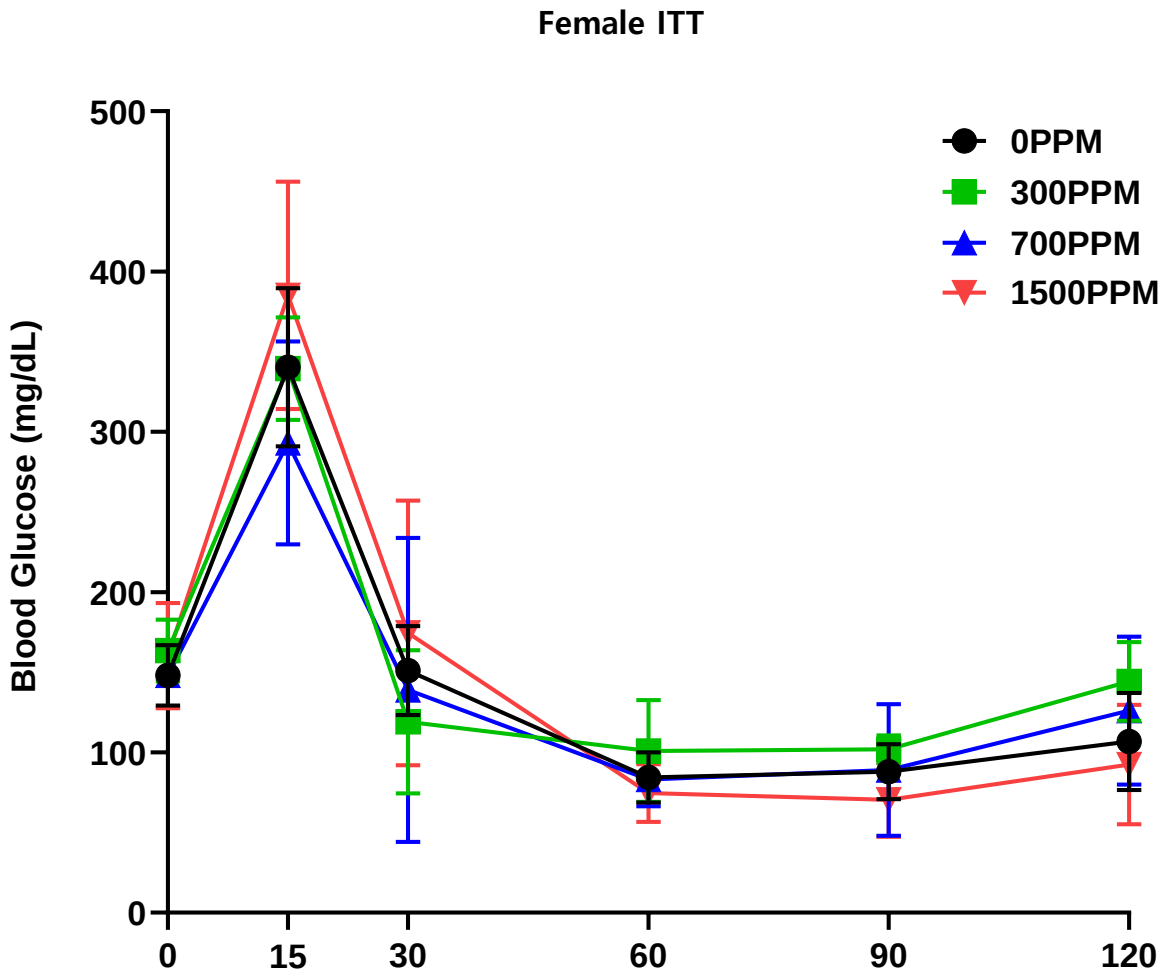

Supplementary Fig. 41

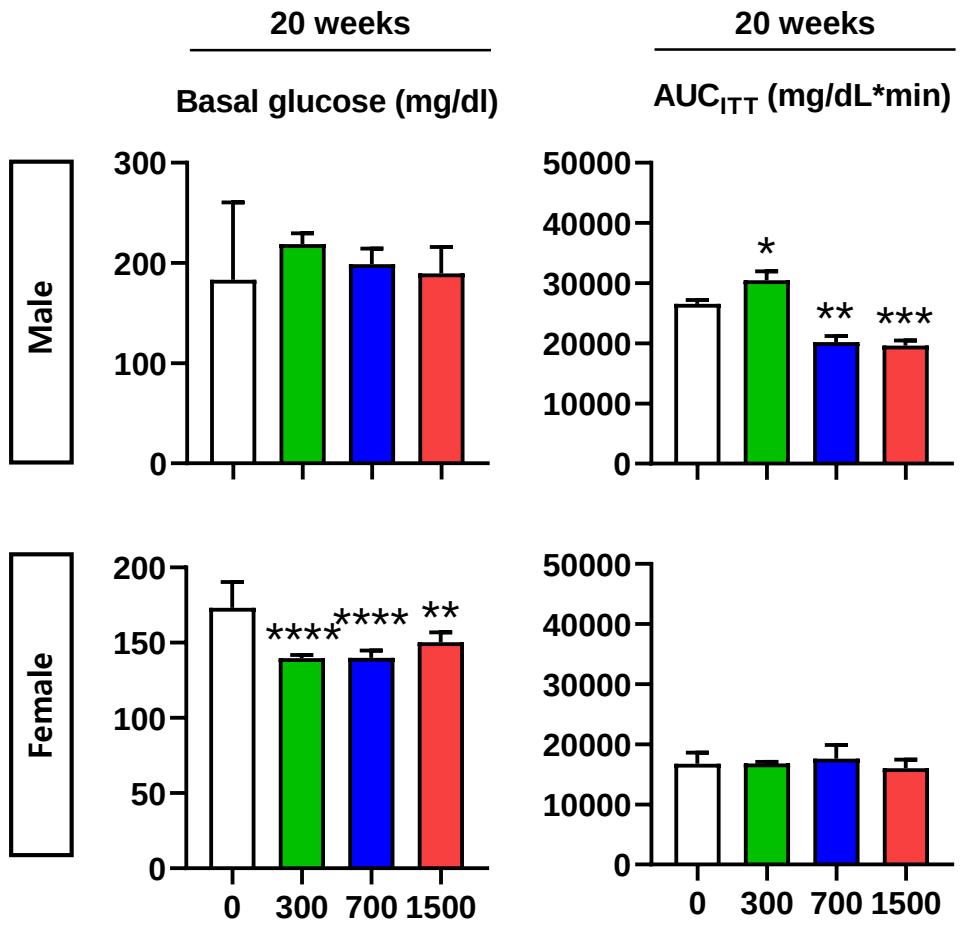

Supplementary Fig. 42

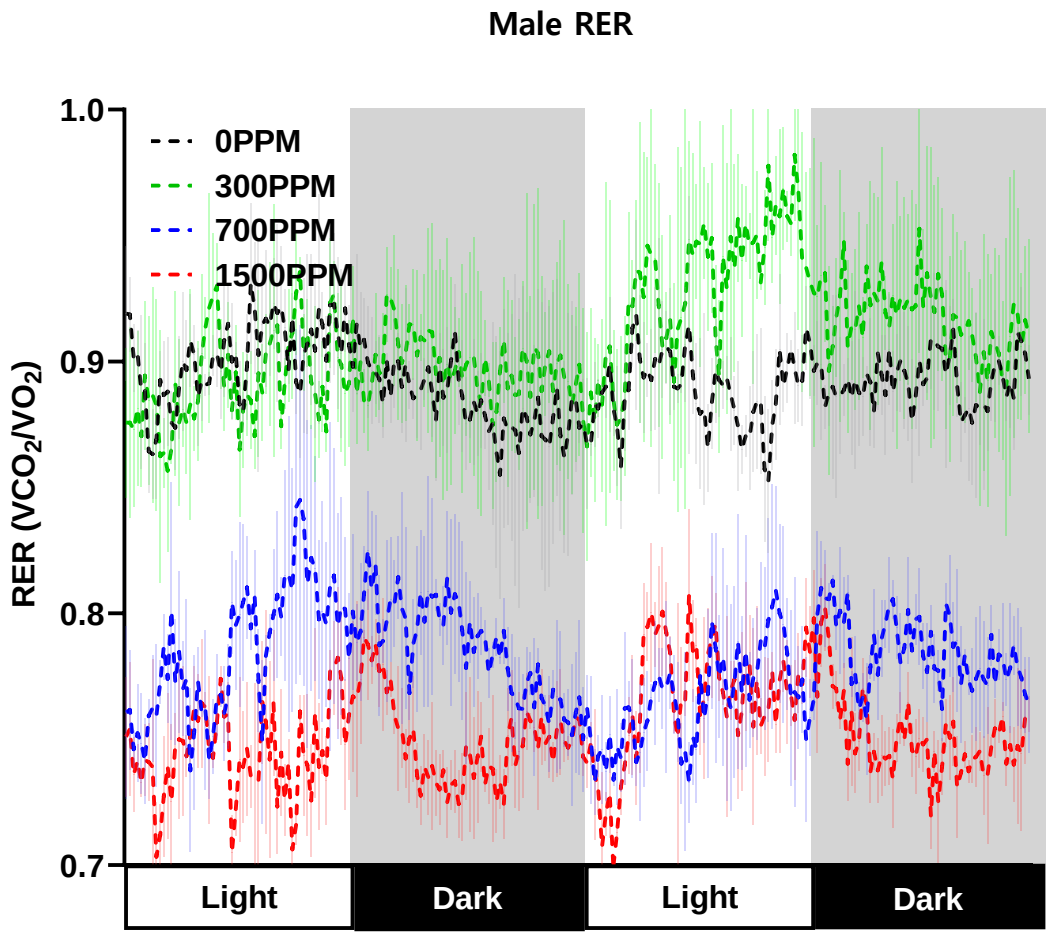

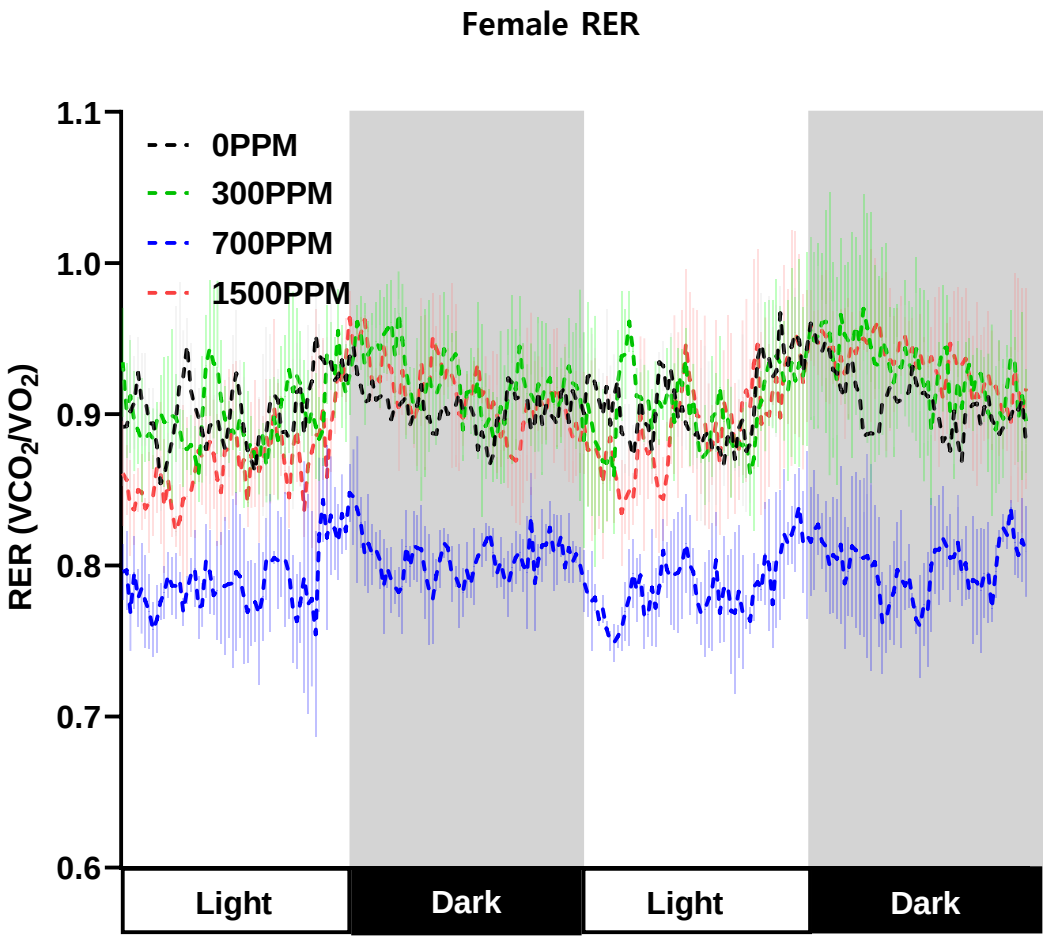

Supplementary Fig. 43

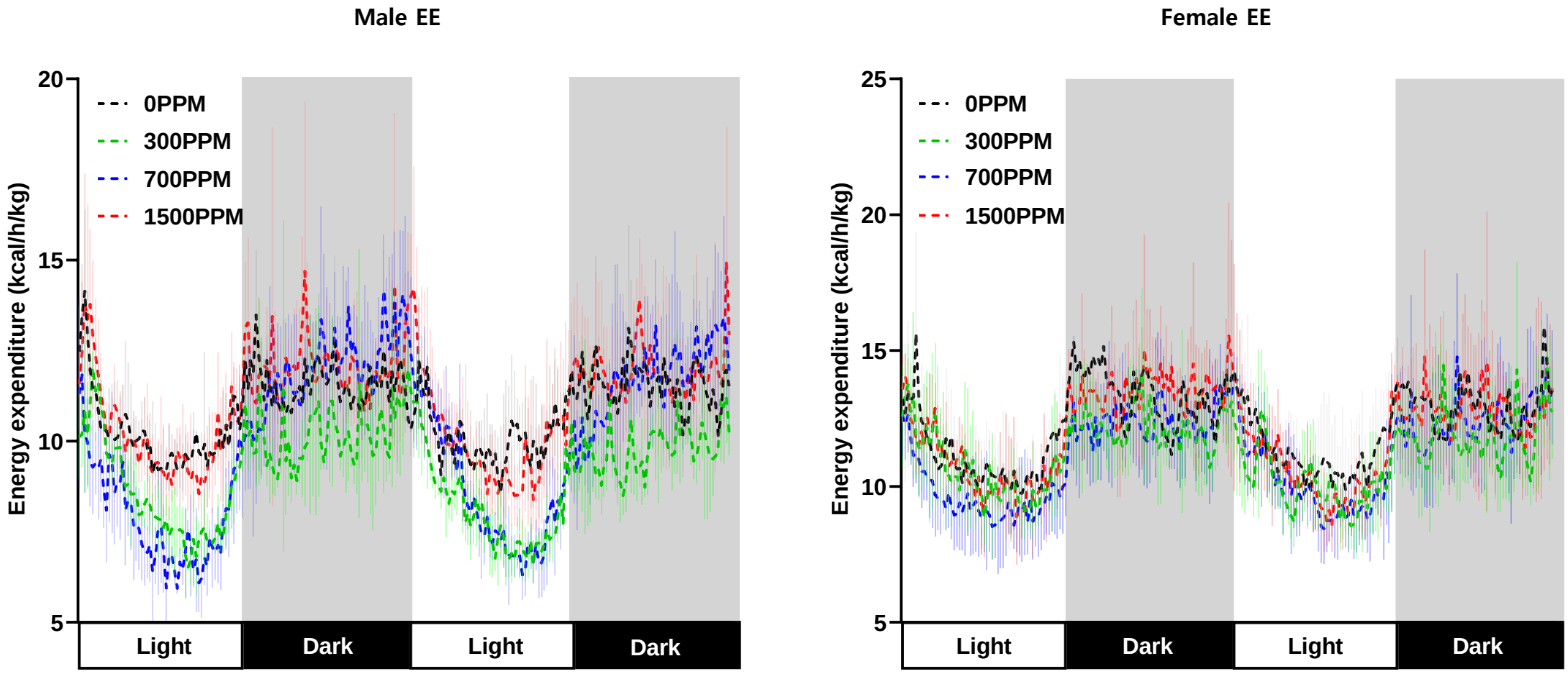

Supplementary Fig. 44

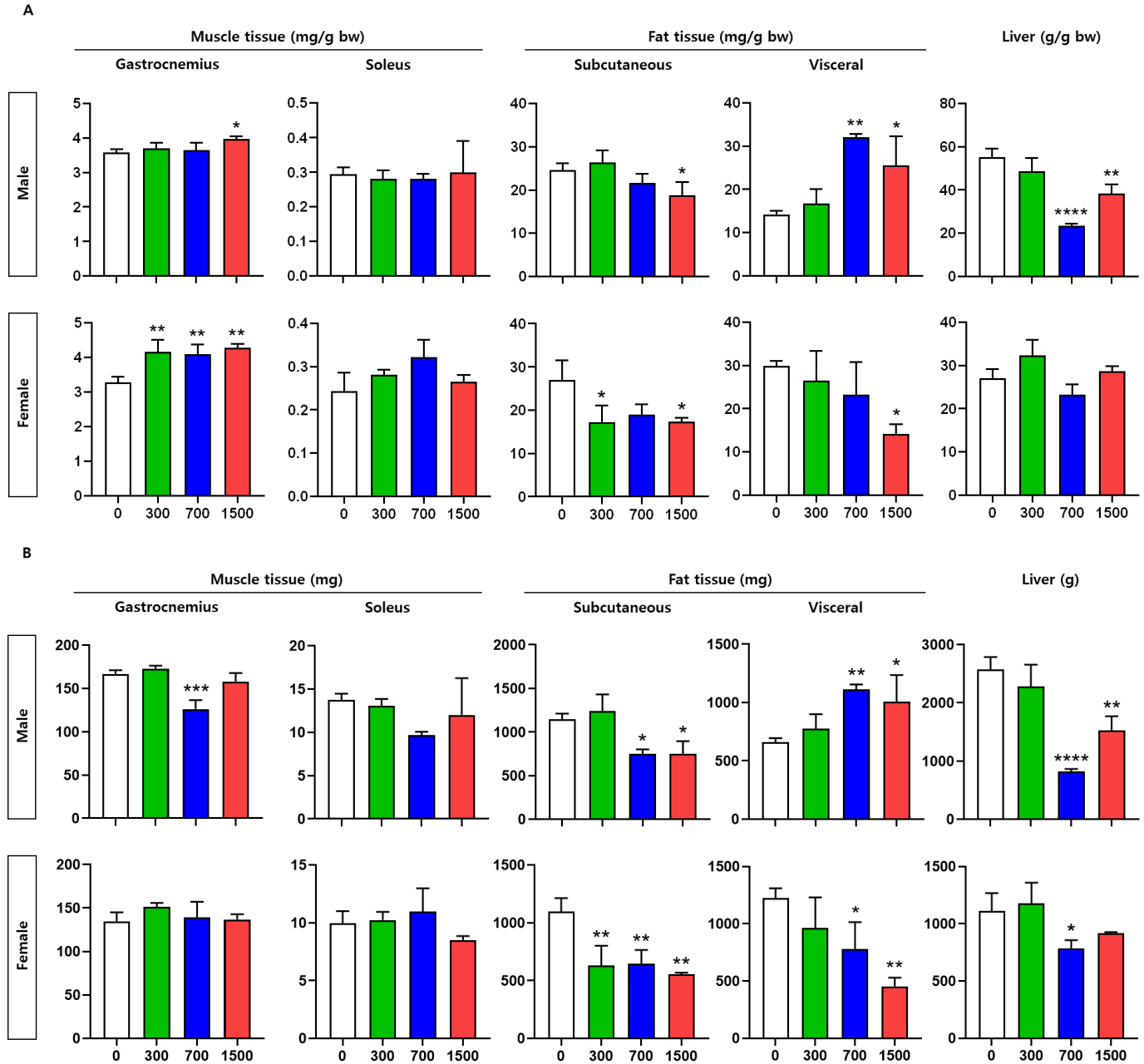

Supplementary Fig. 45

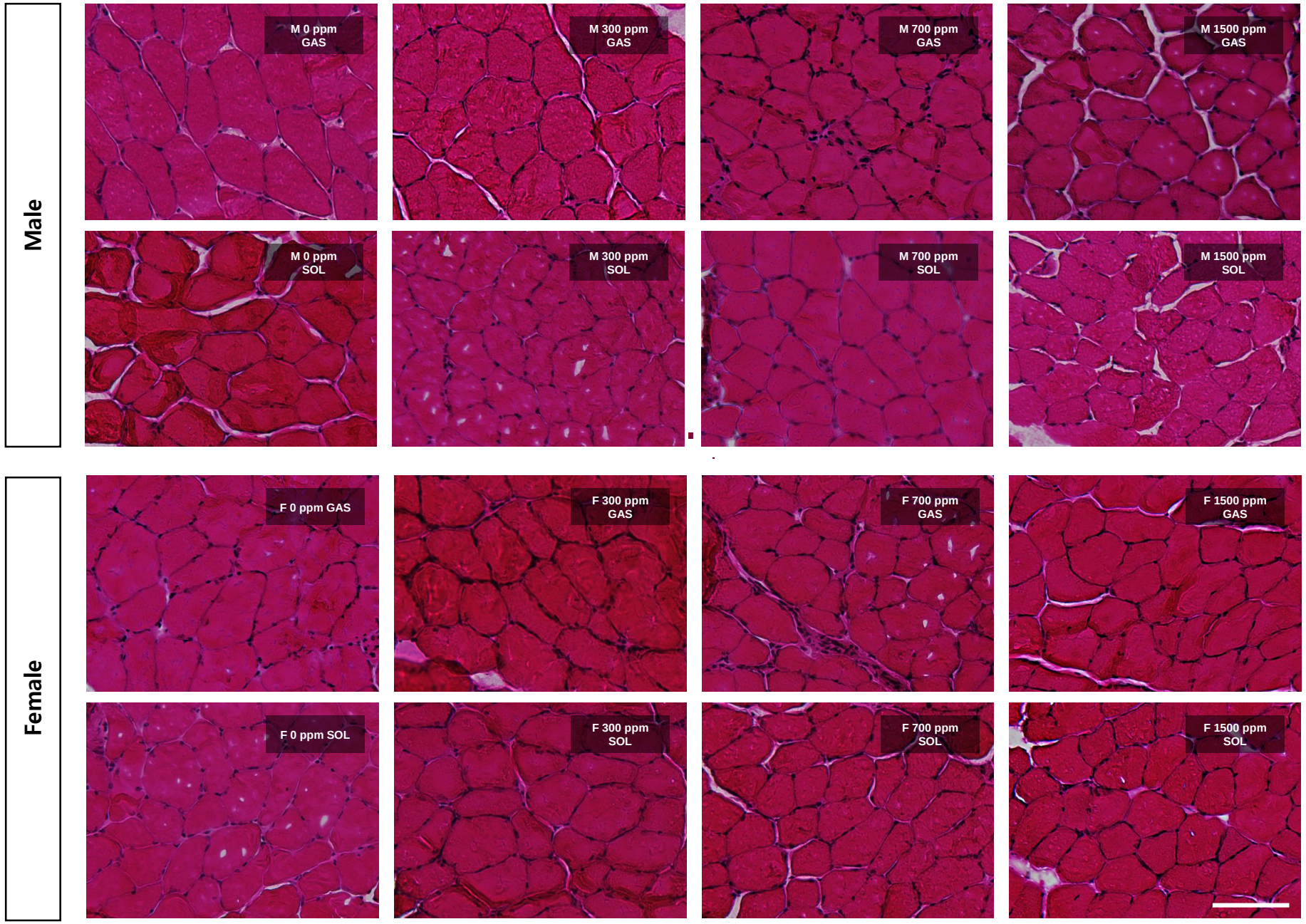

Supplementary Fig. 46

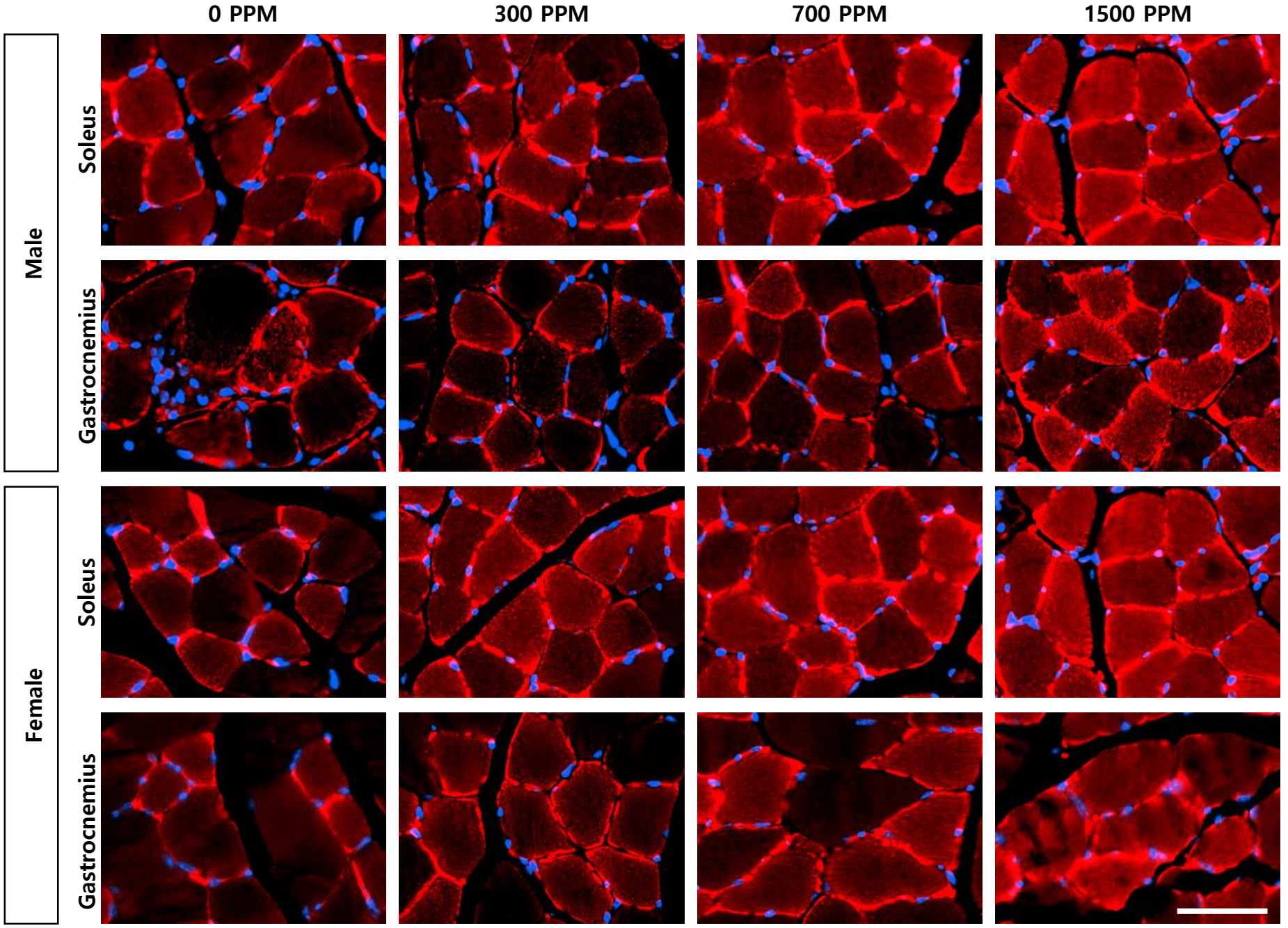

Supplementary Fig. 47

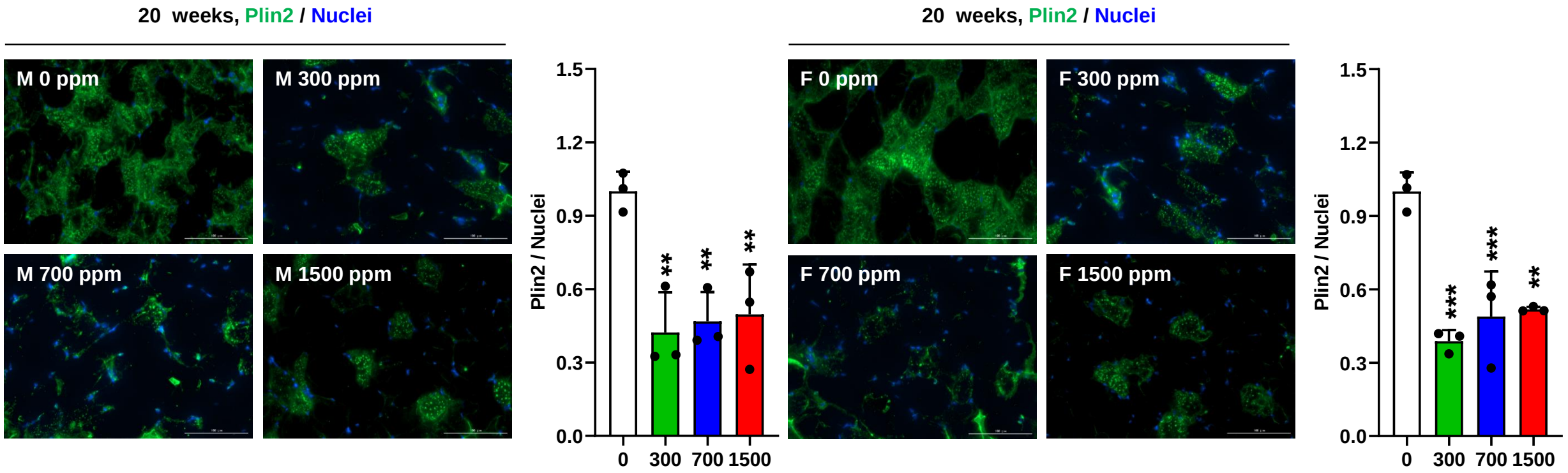

Supplementary Fig. 48

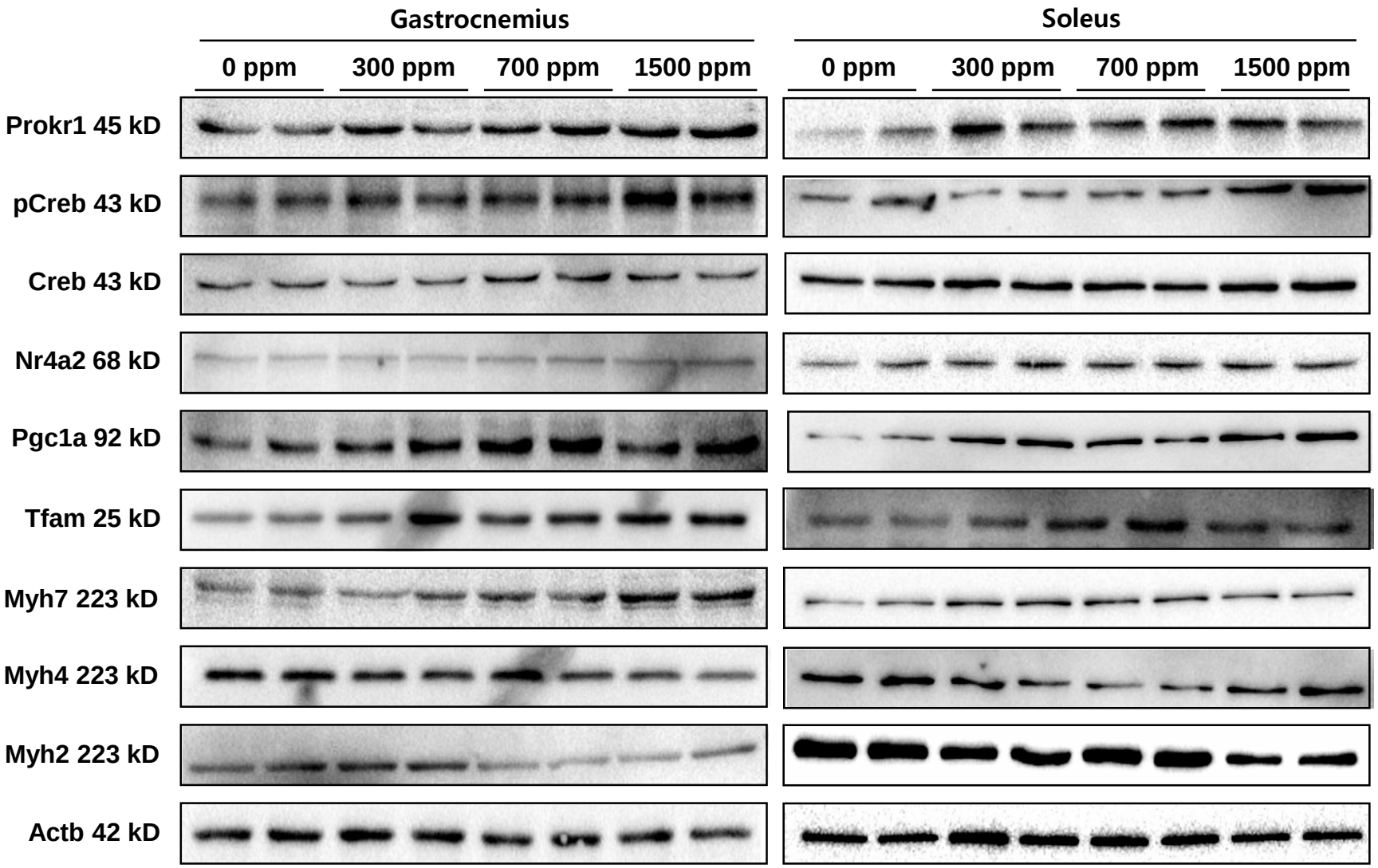

Supplementary Fig. 49